

RESEARCH ARTICLE

Microglia are involved in regulating histamine-dependent and non-dependent itch transmissions with distinguished signal pathways

Yuxiu Yang^{1,2} | Bin Mou^{1,2} | Qi-Ruo Zhang² | Hong-Xue Zhao^{1,2} | Jian-Yun Zhang² | Xiao Yun² | Ming-Tao Xiong² | Ying Liu² | Yong U. Liu³ | Haili Pan² | Chao-Lin Ma² | Bao-Ming Li^{2,4} | Jiyun Peng^{1,2} 

¹School of Basic Medical Sciences, Nanchang University, Nanchang, China

²Institute of Life Science, Nanchang University, Nanchang, China

³Laboratory for Neuroimmunology in Health and Disease, Guangzhou First People's Hospital, School of Medicine, South China University of Technology, Guangzhou, China

⁴Department of Physiology and Institute of Brain Science, School of Basic Medical Sciences, Hangzhou Normal University, Hangzhou, China

Correspondence

Jiyun Peng, Center for Neuropsychiatric Disorders, Institute of Life Science, Nanchang University, 999 Xuefu Road, Honggutan New District, Nanchang, Jiangxi Province, 330031, China.

Email: pengjy@ncu.edu.cn

Funding information

Jiangxi Province "2000 talent" plan, Grant/Award Number: jxsq2018106039; National Natural Science Foundation of China, Grant/Award Numbers: 32060199, 82071245, 31971035, 31771182; Natural Science Foundation of Jiangxi Province, Grant/Award Numbers: 20224ACB206016, 20171ACB20002

Abstract

Although itch and pain have many similarities, they are completely different in perceptual experience and behavioral response. In recent years, we have a deep understanding of the neural pathways of itch sensation transmission. However, there are few reports on the role of non-neuronal cells in itch. Microglia are known to play a key role in chronic neuropathic pain and acute inflammatory pain. It is still unknown whether microglia are also involved in regulating the transmission of itch sensation. In the present study, we used several kinds of transgenic mice to specifically deplete CX3CR1+ microglia and peripheral macrophages together (whole depletion), or selectively deplete microglia alone (central depletion). We observed that the acute itch responses to histamine, compound 48/80 and chloroquine were all significantly reduced in mice with either whole or central depletion. Spinal c-fos mRNA assay and further studies revealed that histamine and compound 48/80, but not chloroquine elicited primary itch signal transmission from DRG to spinal Npr1- and somatostatin-positive neurons relied on microglial CX3CL1-CX3CR1 pathway. Our results suggested that microglia were involved in multiple types of acute chemical itch transmission, while the underlying mechanisms for histamine-dependent and non-dependent itch transmission were different that the former required the CX3CL1-CX3CR1 signal pathway.

KEYWORDS

c-fos, CX3CR1, histamine, itch, microglia, Nppb, TRPV1

1 | INTRODUCTION

Pruritoceptive itch is an unpleasant sensation that is initiated from the skin and elicits a desire to scratch (Yosipovitch et al., 2003). Many kinds of stimuli upon or beneath skin can evoke itch sensation, such as a slight mechanical stroke, particular types of chemicals and inflammation-induced cytokines. Histamine (HA) is one of the most well-known itch mediators that act on H1 and H4 receptors at the

free-ending of pruriceptive nerve fibers (Dong & Dong, 2018; Kashiba et al., 1999; Strakhova et al., 2009). There are also several kinds of non-histamine itch mediators that used on laboratory animal studies, such as chloroquine (CQ), serotonin (5-HT), β -alanine and so on (Dong & Dong, 2018). Similar to pain sensation, chemical itch signals are known to be conveyed by unmyelinated C fibers (Ringkamp et al., 2011; Schmelz et al., 1997; Shim & Oh, 2008). Different groups of Dorsal Root Ganglion (DRG) neurons respond to those stimuli.

Using single-cell RNA sequencing data, the DRG neurons could be categorized into 11 subpopulations. Among them, three non-peptidergic (NP) groups were associated with itch: NP1 expressing MrgprD responds to β -alanine, NP2 expressing MrgprA3 responds to several kinds of mediators including CQ, HA and BAM8-22, and NP3 expressing brain natriuretic peptide (BNP) and somatostatin (SST) responds to HA (Usoskin et al., 2015). Although itch and pain share some common peripheral afferent pathways and influence each other (Davidson & Giesler, 2010; Simone et al., 2004), the spinal-level transmission pathways are quite different. Studies have revealed that itch transmission relies more on neuropeptides release rather than glutamate release from the peripheral neurons (Liu et al., 2010). Neuropeptides that were found to anticipate in itch signal transmission include gastrin-releasing peptide (GRP), natriuretic polypeptide B (Nppb), neuromedin B (NMB), SST, substance P, et al. (Akiyama et al., 2014; Huang et al., 2018; Mishra & Hoon, 2013; Wan et al., 2017).

Peripheral immune cells play important roles on chemical prurito-gen insult detection and chronic itch development (Pasparakis et al., 2014). Mast cells are the major endogenous HA source (Rao & Brown, 2008). Type 2T helper (Th2) cells, macrophages or dendritic cells and infiltrated monocytes are involved in cytokine release, including IL-4, IL-13 and IL-31 (Brandt & Sivaprasad, 2011; Nattkemper et al., 2018; Oetjen et al., 2017). Despite the well-known involvement of immune system in the periphery, whether immune cells participate in the central transmission of itch sensation is largely unknown.

Microglia are the resident immune cells in the central nerve system (CNS). Microglia share many properties with peripheral macrophages (e.g., expression of CX3CR1), but are originated from different sources during early development (Gomez Perdiguero et al., 2015). A bunch of studies have revealed that microglia are one of the key players in pain hypersensitivity and chronic pain development (Inoue & Tsuda, 2018; Peng et al., 2016). With peripheral nerve injury, spinal microglia would be activated by multiple signals, including the fractalkine or CX3CL1 signals, through CX3CR1 receptors, ATP/ADP signals through purinergic receptors such as P2X4, P2X7 and P2Y12, and the CSF1 signals. These signal pathways are thought to be involved in microglial-promoting pain hypersensitivities. To study whether microglia and peripheral resident macrophages are involved in acute itch sensation, and what is the signal pathway, we used multiple transgenic tools to deplete microglia and peripheral macrophages together (whole depletion) or deplete microglia alone (central depletion), and examined how itch responses that induced by either HA dependent or non-dependent insults were affected. We demonstrated that microglia were involved in both HA-dependent and non-dependent (CQ) itch transmission. Further Spinal c-fos mRNA assay and behavior screening studies with the P2Y12 KO and CX3CR1 KO mice revealed that the underlying mechanisms for HA-dependent and non-dependent itch transmission are different that the former requires the CX3CL1-CX3CR1 signal pathway, while the latter does not. The microglial P2Y12 receptors are not involved in any acute itch signal transmission.

2 | RESULTS

2.1 | Depletion of CX3CR1+ microglia and macrophages inhibited acute itch responses to HA, C48/80 and CQ

The CX3CR1 fractalkine receptors are highly expressed in central microglia and peripheral macrophages. To establish an overall effect of CX3CR1+ cell depletion on acute itch transmission, we first used the CSF1R^{f/f};CX3CR1^{CreER/+} transgenic mice to knock out the csf1r gene in all CX3CR1+ cells. Because the CSF1 receptors in microglia and macrophages are essential for cell survival (Elmore et al., 2014; MacDonald et al., 2010), knock out of the gene will cause cell apoptosis. With three doses of tamoxifen (TM, 150 mg/kg, i.p., 48 h interval) treatment, 98.4 \pm 1.1% of microglia in the spinal cord and 80.6 \pm 2.9% of macrophages in the DRG were depleted when checked at 24 h after the last Tamoxifen injection. While in the skin of the back neck, the number of F4/80+ labeled dendritic cell was not affected (Figure 1a,b). Thus, the CSF1R strategy efficiently depleted the central microglia and the DRG macrophages but did not affect peripheral dendritic cells.

To examine the effect of microglia and macrophage depletion on acute itch transmission, we first tested the itch responses in the HA model and the HA-dependent compound 48/80 model in the depletion mice and the control CSF1R^{f/f} mice that received the same doses of TM treatment. In the HA model, the behavioral responses (19.64 \pm 2.588 scratch bouts within 30 min) of the depletion mice were significantly less than that of the control mice (51.70 \pm 4.069 scratch bouts within 30 min, Figure 1c). The C48/80 is a very strong itching mediator that act on mast cells and cause degranulation and HA release (McNeil et al., 2015). The scratch responses to C48/80 were much stronger than that to HA treatment in the normal control mice. The scratch frequencies were progressively increased after 3 min and reached the peak within 15 min (Figure S1A). Thus, we separated the total 30 min scratch responses as early stage (0–3 min) and late stage (3–30 min). As shown in Figure 1c, in the depletion mice, the scratch bouts were significantly decreased in both the early stage ($p = .040$) and the later stage ($p = .00011$), and for the total bout counts as well ($p = .000107$, Figure S3A). The results suggested that the HA-dependent itch responses required the CX3CR1+ cells.

We then examined another HA non-dependent model, the CQ model, which induces strong itch responses. CQ treatment in the normal control mice is characterized by typical two-phase responses. The mice began scratching immediately after the CQ injection and then calmed down briefly in 3 min. After that, the scratch frequencies increased progressively and reach the peak at around 15 min (Figure S1B). In the depletion mice, as shown in Figure 1c, the scratch bouts were significantly less than the control in both the early ($p = .0049$) and late ($p < .0001$) stages, and for the total bout counts as well ($p < .0001$, Figure S3A). The results suggested that the non-histamine-dependent itch responses to CQ also required the CX3CR1+ cells.

We also examined the itch responses to β -alanine and mechanical stimulus. β -alanine is a relatively weaker pruritoceptive mediator compared with C48/80 and CQ that the signal is

relayed by the NP1 type DRG neurons. Interesting, the scratch responses to β -alanine injection to neck skin in the depletion mice were comparable to that in the control mice ($p = .834$)

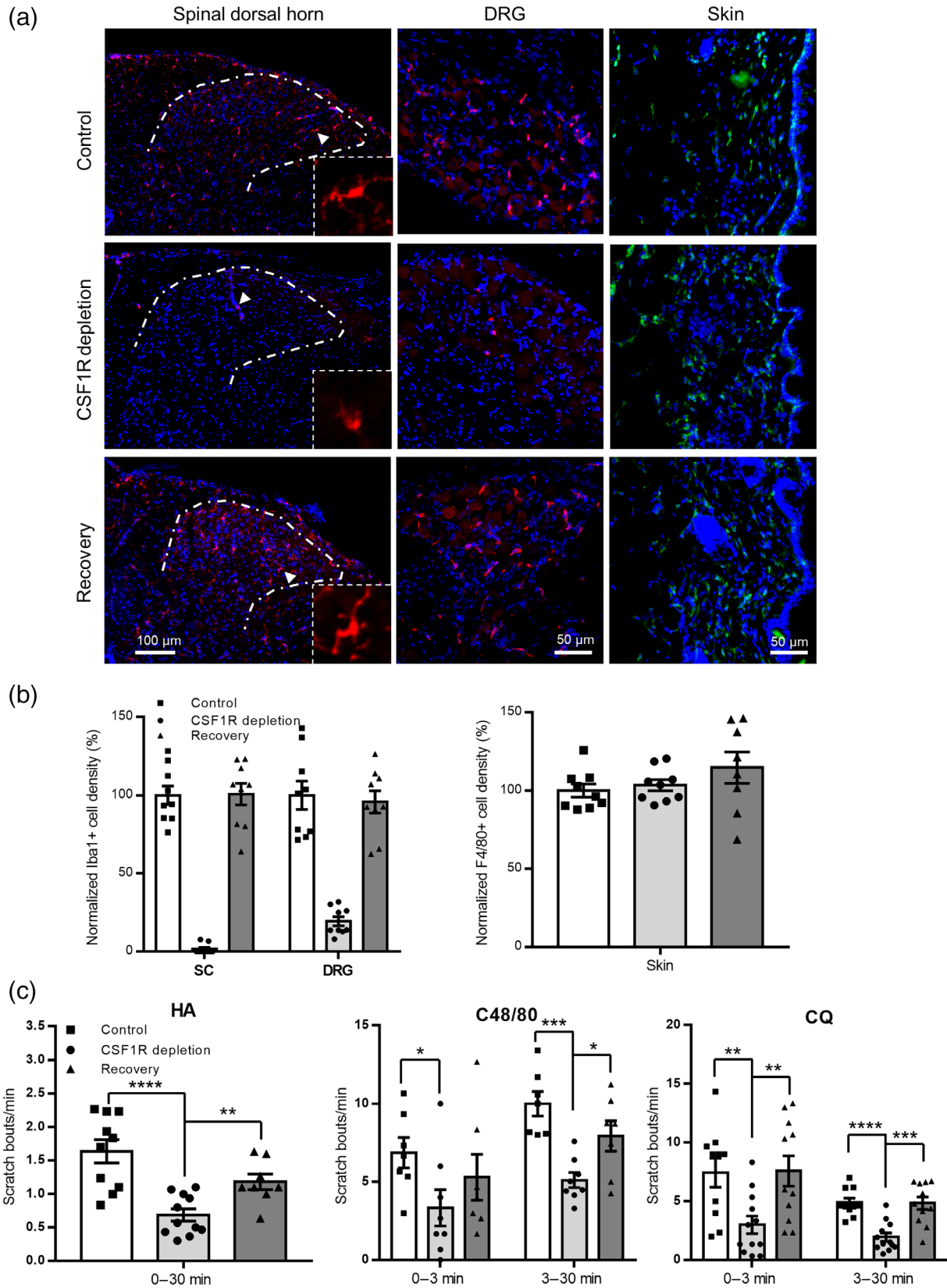


FIGURE 1 Legend on next page.

(Figure S2A). Therefore, β -alanine-induced itch sensation transmission did not require microglia or macrophages.

For the mechanical itch test, the mechanical stimuli on the skin behind the ear were applied using the Von Frey filaments ranging from 0.02 to 0.4 g. Similar to previous reported (Pan et al., 2019), the normal control mice were most sensitive to 0.07 g (0.7 N) stimulus. In the depletion mice, the scratch responses to all the tested stimulus strengths were similar to that in the controls, respectively ($p = .544$ for group effect with two-way ANOVA, repeated measurement) (Figure S2B). Therefore, mechanical stimuli-induced itch sensation transmission did not require microglia or macrophages.

With the above pruritoceptive reagents screening tests, we concluded that the CX3CR1⁺ microglia and/or macrophages were involved in the itch sensation transmission that was elicited by agents depending on HA pathway and the HA non-dependent agent, CQ. The non-affected itch responses to β -alanine and mechanical stimuli suggested that the microglia/macrophage depletion did not affect the behavioral presentation of itch responses.

To further confirm whether the transient microglia/macrophage depletion affect the itch transmission pathway in a long term, we did the second tests in the depletion mice for the HA, C48/80 and CQ model at 14 days after the first test (recovery group in Figure 1). During the 14 days, no further TM was injected. Thus, microglia and macrophages were repopulated and reached the pre-ablation level (Figure 1a,b). The results showed that, for all the three models the scratch responses in the mice recovered from the microglia/macrophages depletion were restored and comparable to that in the controls, respectively (Figure 1c). Therefore, the transient microglia/macrophage depletion would not disrupt itch transmission circuits permanently.

2.2 | Depletion of central microglia inhibited acute itch responses to HA, C48/80 and CQ

Since the CSF1R conditional knockout strategy depleted microglia and macrophages at the same time, we could not distinguish the role of central microglia from peripheral macrophages. To dissect the exact role of microglia in itch transmission, we used the ROSA^{tdTomato/+}; CX3CR1^{CreER/+} to ablate microglia alone. The hematopoietic

originated monocytes/macrophages have a quick turn-over rate. Several weeks after TM treatment, the circulating monocytes and part of tissue macrophages would be replaced by new cells originated from hematopoietic stem cells (HSCs). Since HSCs do not express CX3CR1, the new cells would not express the induced diphtheria toxin receptors (DTR) and not be affected by the diphtheria toxin treatment (Parkhurst et al., 2013; Peng et al., 2016). Thus, we waited 3 weeks after the TM treatment (150 mg/kg, i.p., four doses with 48 h interval), then two doses of DT (0.75 μ g per mice with 48 h interval, i.p.) were given. One day after the second DT injection, 76.3 \pm 5.3% of Iba1⁺ cells in the spinal cord were ablated, while 37.9 \pm 7.5% of Iba1⁺ cells in the DRG were ablated as well (Figure 2b). Thus, the central microglia were efficiently ablated, but the peripheral DRG macrophages were partially ablated as well.

To separate the central microglia from the peripheral macrophages/monocytes more clearly. We further used the TMEM119-CreER transgenic mouse to generate the TMEM119^{CreER/+}; ROSA^{tdTomato/+} mice. Tmem119 gene was found to be specifically expressed in central microglia only (Satoh et al., 2016). We confirmed the tmem119 expression pattern with the TMEM119^{CreER/+}; ROSA^{tdTomato/+} mice. With 5 doses of TM injection (100 mg/kg with 24 h interval, i.p.), The tdTomato expression were successfully induced in around 90% of Iba1⁺ spinal microglia cells, but almost none in Iba1⁺ DRG macrophages (Figure S4). With a series of pilot tests, we finally chose a 10-dose TM (150 mg/kg with 24 h interval, i.p.) injection protocol to achieve a reliable microglia depletion efficiency. Six days after the last TM injection, two doses of DT (0.75 μ g per mice with 48 h interval, i.p.) were injected to ablate microglia cells. As shown in Figure 2a,b, Iba1⁺ cells were reduced by 42.2 \pm 1.8% of control in the spinal cord. Most of the remained microglia cells showed ramified morphology similar to the WT control, suggesting that those cells were not affected by DT and the TM-induced gene modification was not succeeded in the remained microglia cells. The Iba1⁺ cells in the DRG were comparable to that of the control mice ($p = .716$). Therefore, using the TMEM119-CreER tools, we could specifically manipulate microglia without affecting the peripheral macrophages, although the efficiency was less than that of the CX3CR1-CreER.

To examine how the acute itch transmission was affected by microglia depletion. We tested the acute itch responses in both the DT-treated

FIGURE 1 CSF1R depletion inhibited acute itch responses to HA, C48/80 and CQ. (a, b) With tamoxifen (TM) treatment, the Iba1⁺ microglia cells in spinal cord (SC) and macrophage cells in dorsal root ganglion (DRG) of the CSF1R^{f/f}; CX3CR1^{CreER/+} mice were reduced to 1.6 \pm 1.1% and 19.4 \pm 2.9% of basal levels, respectively. While the F4/80⁺ dendritic cells in the skin were not altered. The recovery samples were obtained 15 days after the last TM injection. Iba1⁺ cells in both SC ($p = .938$, un-paired t-test) and DRG ($p = .721$) were returned to control levels ($n = 3$ mice for each group, CSF1R^{f/f} mice were used as control and received the same doses of TM). The arrow indicated cells were enlarged at the bottom-left to show the morphology. (c) Scratch responses over 30 min with HA (50 μ g in 10 μ L saline), C48/80 (100 μ g in 50 μ L saline) and CQ (200 μ g in 50 μ L saline) injected into nape, respectively. CSF1R depletion significantly decreased the scratch responses to HA ($n = 10$ for control, $n = 11$ for CSF1R depletion, $p < .0001$) during the 30 min observation; decreased the responses to C48/80 at both the early (0–3 min, $p = .040$) and late (3–30 min, $p = .00011$) stages ($n = 7$ for control, $n = 8$ for CSF1R depletion); decreased the responses to CQ at both the early ($p = .0049$) and late ($p < .0001$) stages ($n = 10$ for control, $n = 12$ for CSF1R depletion). The secondary test after microglia recovery were done 14 days after the first one with the same agents. The responses to HA ($n = 8$, $p = .055$), C48/80 ($n = 7$, $p = .390$ for 0–3 min, $p = .125$ for 3–30 min) and CQ ($n = 11$, $p = .938$ for 0–3 min, $p = .941$ for 3–30 min) were all back to control levels, respectively. * $p < .05$, ** $p < .01$, *** $p < .001$, **** $p < .0001$, un-paired t-test. Data were presented as mean \pm SEM.

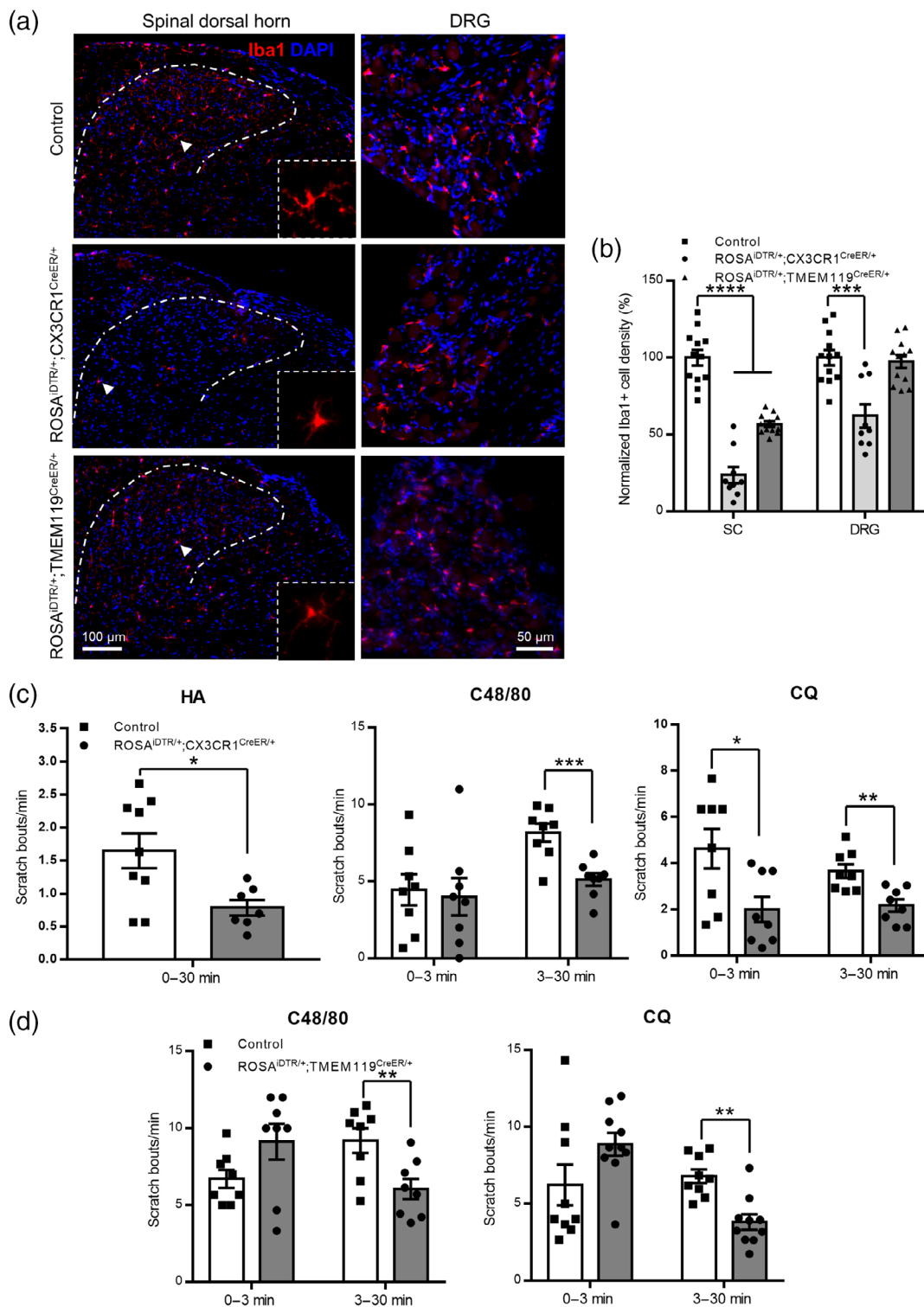


FIGURE 2 Central microglia ablation inhibited acute itch responses to HA, C48/80 and CQ. (a, b) With two doses of Diphtheria Toxin (DT, i.p., 0.75 μg in 200 μL PBS per injection, 48 h interval) treated to the TM pre-treated ROSA^{IDTR/+};CX3CR1^{CreER/+} and ROSA^{IDTR/+};TMEM119^{CreER/+} mice, microglia cell densities in the SC were reduced to 23.7 ± 5.3% ($p < .0001$) and 56.8 ± 1.8% ($p < .0001$) of control level, respectively; in the DRG, the Iba1+ macrophages were reduced to 62.1 ± 7.5% in the CX3CR1-CreER mice ($p = .00031$), and were not affected in the TMEM119-CreER mice ($p = .709$). ($n = 3$ mice for each group, ROSA^{IDTR/+} mice were used as control and received the same doses of TM and DT, respectively). Arrow indicated cells were enlarged in the bottom right corners. (c) Microglia ablation in the ROSA^{IDTR/+};CX3CR1^{CreER/+} mice significantly reduced the scratch responses to HA ($n = 9$ for control, $n = 7$ for ablation, $p = .017$) during the 30 min observation; reduced the responses to C48/80 at the late ($p = .00073$), but not early ($p = .775$) stage ($n = 8$ for control, $n = 8$ for ablation); reduced the responses to CQ at both the early ($p = .0217$) and late ($p = .0026$) stages ($n = 8$ for control, $n = 8$ for ablation). (d) Microglia ablation in the ROSA^{IDTR/+};TMEM119^{CreER/+} mice significantly reduced the scratch responses to C48/80 at the late ($p = .0091$), but not early ($p = .085$) stage ($n = 8$ for control, $n = 8$ for ablation); reduced the responses to CQ at the late ($p = .00038$), but not early ($p = .092$) stage ($n = 9$ for control, $n = 10$ for ablation). * $p < .05$, ** $p < .01$, *** $p < .001$, un-paired t -test. Data were presented as mean ± SEM.

$ROSA^{iDTR/+};CX3CR1^{CreER/+}$ and $ROSA^{iDTR/+};TMEM119^{CreER/+}$ mice (Figure 2c,d). With HA treatment, the total scratch bouts within 30 min in the $ROSA^{iDTR/+};CX3CR1^{CreER/+}$ ($p = .017$) mice were significantly less than that of the control group, which received the same doses of TM and DT treatments. With C48/80 treatment, the scratch responses in the early stage (0–3 min) were not altered in both the $ROSA^{iDTR/+};CX3CR1^{CreER/+}$ ($p = .775$) and $ROSA^{iDTR/+};TMEM119^{CreER/+}$ ($p = .085$) mice compared to each control group, but the scratch responses in the late stage (3–30 min) were significantly decreased in both the $ROSA^{iDTR/+};CX3CR1^{CreER/+}$ ($p = .0007$) and $ROSA^{iDTR/+};TMEM119^{CreER/+}$ ($p = .0091$) mice compared to each control group, and the total scratch responses in 30 min were decreased in both groups as well ($p = .00123$ and $.0209$, respectively, Figure S3B and S3C). With CQ treatment, the scratch responses in the early stage (0–3 min) were significantly decreased in the $ROSA^{iDTR/+};CX3CR1^{CreER/+}$ ($p = .0217$) but not $ROSA^{iDTR/+};TMEM119^{CreER/+}$ ($p = .092$) mice compared to each control group, and the scratch responses in the late stage (3–30 min) were significantly decreased in both the $ROSA^{iDTR/+};CX3CR1^{CreER/+}$ ($p = .0026$) and $ROSA^{iDTR/+};Tmem119^{CreER/+}$ ($p = .0004$) mice compared to each control group, and the total scratch responses in 30 min were decreased in both groups as well ($p = .00126$ and $.00183$, respectively, Figure S3B and S3C). The results suggested that microglia were involved in the HA dependent and non-dependent (CQ) acute itch transmission. The different impact on the early-stage responses among the CSF1R depletion strategy and the two kinds of iDTR strategy suggested that the peripheral macrophages could also contribute to both the HA dependent and non-dependent acute itch transmission, at least in the early stage.

To further examine whether microglia were involved in chronic itch, we used a 8-day acetone-ether-water (AEW) dry skin model to test how the spontaneous itch behaviors were affected by microglia depletion in the $ROSA^{iDTR/+};CX3CR1^{CreER/+}$ mice. Both the depletion and control group were treated with AEW for 4 days before the DT injection to allow an initial chronic itch development. As shown in Figure S3F, the two groups developed a similarly low level of spontaneous itch on day 2 and day 4 ($n = 9$ mice for both groups). The control group further increased the scratch bouts on day 6 and day 8 ($p = .0143$ for day 6 vs. day 4, $p = .0004$ for day 8 vs. day 6, paired t -test). However, in the microglia depletion group, the itch behaviors at day 6 and day 8 were remained at a similar level as day 4 ($p = .313$ for day 6 vs. day 4, $p = .220$ for day 8 vs. day 4, paired t -test), and were significantly less than those in the control group ($p = .0197$ for day 6 and $p = .0002$ for day 8, unpaired t -test). Therefore, microglia were also involved in the dry skin-induced chronic itch.

2.3 | Microglia were involved in the primary HA, but not CQ itch signal transmission from DRG to spinal cord

To dissect how microglia regulated the neuronal circuits for itch in the spinal level, we examined the *c-fos* mRNA expression changes at 90 min after the itch agent application via RNAscope. The spinal Npr1+ inter-neurons were known to directly receive both

HA-dependent and non-dependent itch signals from DRG primary projection (Fatima et al., 2019; Mishra & Hoon, 2013). And the spinal Sst + inter-neurons that relay inhibiting signal to DYN+ neurons and work as a disinhibiting function for the itch signals, also occupy an up-stream position in the spinal level of itch transmission (Chen & Sun, 2020; Fatima et al., 2019). Therefore, we co-labeled these neurons together with *c-fos*. As expected, with HA, C48/80 and CQ treatment, the *c-fos* positive cell numbers were significantly increased in the cervical spinal dorsal horn of all three WT groups ($p < .0001$ for all three groups compared to naïve) (Figure 3–5). In the $ROSA^{iDTR};CX3CR1^{CreER/+}$ mice with microglia ablation, HA and C48/80 induced *c-fos* up-regulation were significantly inhibited compared with the WT groups, respectively ($p < .0001$ for both) (Figures 3b and 4b). However, CQ-induced total *c-fos* up-regulation was not reduced by microglia ablation ($p = .073$), but the *c-fos* + cell distribution were changed that the *c-fos* + cells clustered in the lateral spinal nucleus (LSN) were significantly reduced ($p < .0001$), where most of the ascending projection neurons were located (Li et al., 2021; Figure 5b). For the Npr1+ neurons, the percentage of *c-fos* + cells were increased from $8.60 \pm 0.66\%$ to $23.50 \pm 2.05\%$ ($p < .0001$) in the HA-treated WT mice (Figure 3c), to $19.85 \pm 1.97\%$ ($p < .0001$) in the C48/80-treated WT mice (Figure 4c), to $26.7 \pm 4.09\%$ ($p < .0001$) in the CQ-treated WT mice (Figure 5c). Microglia ablation significantly decreased HA ($p = .00015$, Figure 3c) and C48/80 ($p = .0021$, Figure 4c), but not CQ ($p = .7460$, Figure 5c) induced *c-fos* expression in the Npr1+ neurons. For Sst + neurons, the percentage of *c-fos* + cells were increased from $6.36 \pm 0.64\%$ to $13.10 \pm 1.21\%$ ($p < .0001$) in HA-treated WT mice (Figure 3c), to $8.56 \pm 0.68\%$ ($p = .0263$) in C48/80-treated WT mice (Figure 4c), to $16.91 \pm 2.38\%$ ($p < .0001$) in CQ-treated WT mice (Figure 5c). Microglia ablation significantly decreased HA ($p = .0315$, Figure 3c) and C48/80 ($p = .0004$, Figure 4c), but not CQ ($p = .2961$, Figure 5c) induced *c-fos* expression in the Sst + neurons as well. To further confirm that the downstream neuronal activity was reduced by microglia ablation in the CQ model, we examine the *c-fos* signal in Grpr+ neuron. As show in Figure S5, CQ elicited *c-fos* expression in Grpr+ cells was significantly reduced by microglia depletion. These results suggested that spinal microglia were involved in the HA-dependent itch signal primary transmission from DRG to the spinal cord, but for the CQ-elicited itch, spinal microglia were only involved in the secondary local signal relay.

2.4 | Spinal CX3CL1-CX3CR1 microglial signal pathway was required for HA dependent, but not CQ elicited itch signal transmission

The above results suggested that spinal microglia were stimulated by very up-stream signals from the HA itch neuronal circuits. Purinergic signal is one of the major components to activate microglia. The P2Y12 receptors are highly expressed in microglia and mediate the microglial process movement toward ATP/ADP gradient (Haynes et al., 2006). Therefore, we first tested the acute itch responses in the

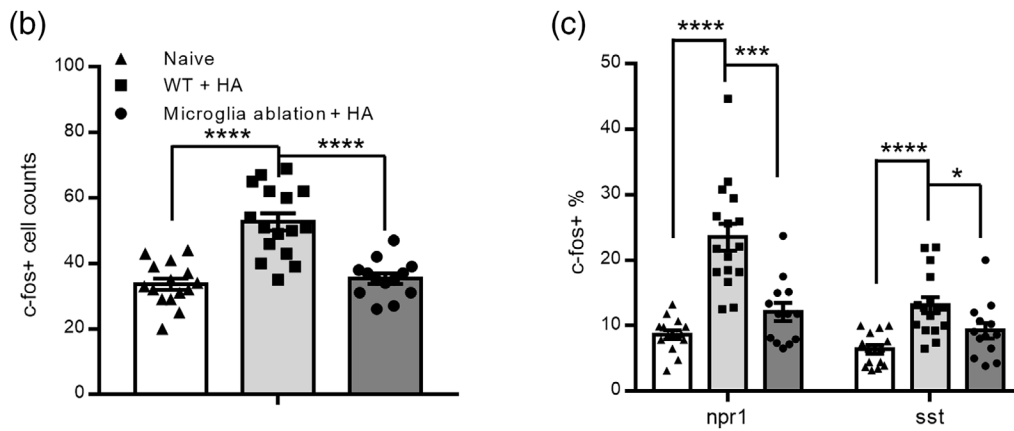
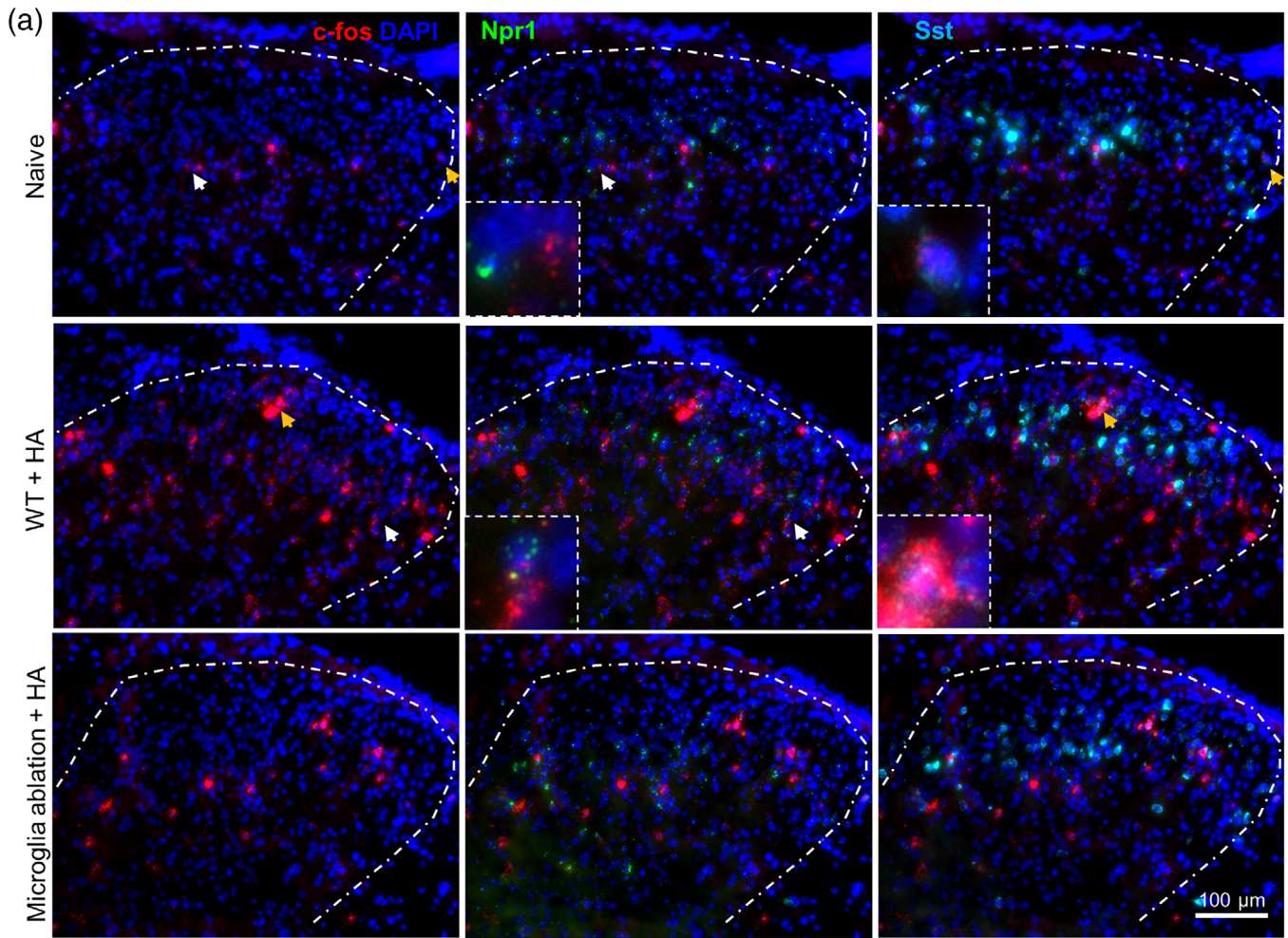


FIGURE 3 HA induced spinal c-fos mRNA expression was reduced in microglia ablation mice. (a) representative RNAscope images showed triple labeling of c-fos, npr-1 and Sst mRNA in the spinal dorsal horn of WT naïve, HA-treated WT and microglia ablation (ROSA^{IDTR};CX3CR1^{CreER/+}) mice. White and orange arrows indicated c-fos + cells were enlarged at the bottom-left of the middle and right panels to show the co-labeling with npr-1 and Sst, respectively. (b, c) Statistic data showed that HA-induced increase of overall c-fos + cell number in WT mice was greatly reduced in the microglia ablation mice ($p < .0001$ for naïve vs. WT + HA and WT + HA vs. ablation + HA), and the increase of c-fos + percentage of Npr1+ and Sst + cells were also significantly reduced (c, $p < .0001$ for naïve vs. WT + HA in both Npr1+ and Sst + cells, $p = .00015$ for WT + HA vs. ablation + HA in Npr1+ cells, $p = .0315$ for WT + HA vs. ablation + HA in Sst + cells). $n = 15, 16$ and 13 images for naïve, WT + HA, and ablation + HA group, respectively. Samples were obtained from three mice for each group. * $p < .05$, *** $p < .001$, **** $p < .0001$, un-paired t -test. Data were presented as mean \pm SEM.

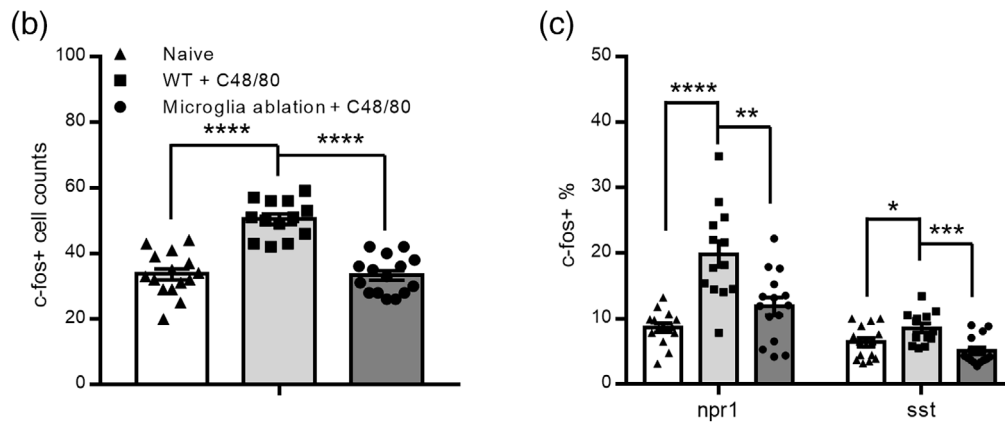
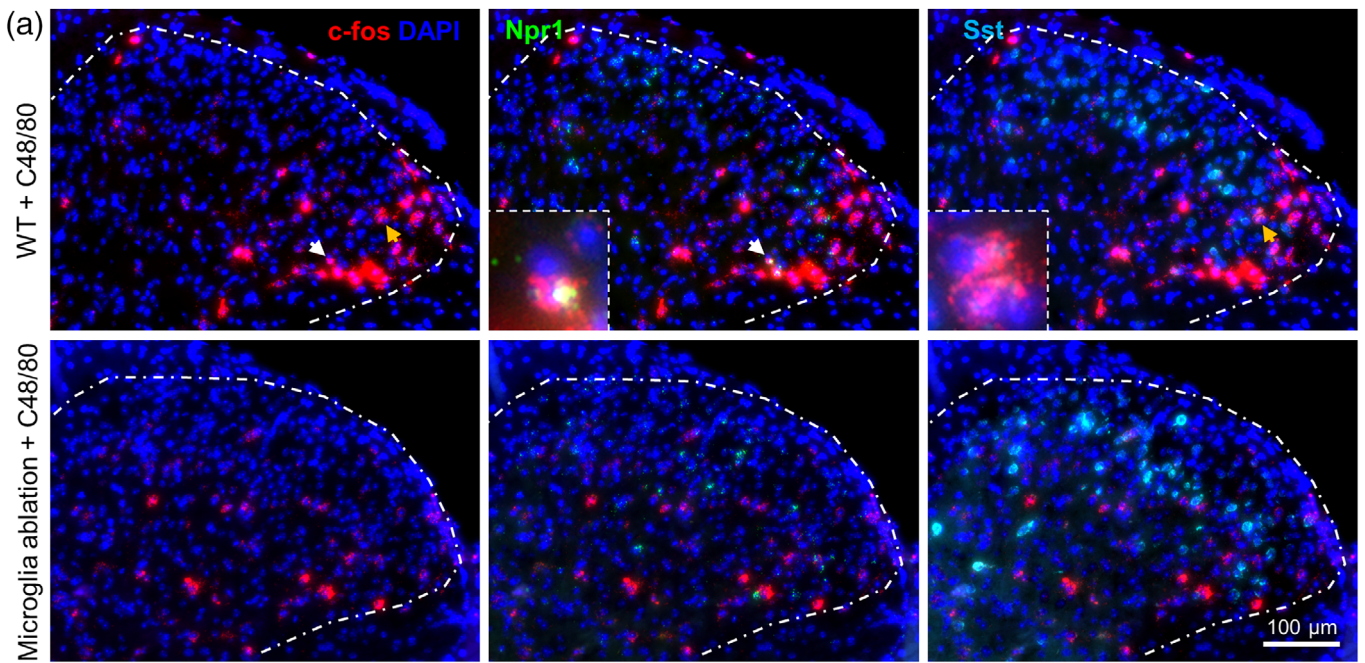


FIGURE 4 C48/80 induced spinal c-fos mRNA expression was reduced in microglia ablation mice. (a) representative RNAscope images showed triple labeling of c-fos, npr-1 and Sst mRNA in the spinal dorsal horn of C48/80 treated WT and microglia ablation ($ROSA^{IDTR}; CX3CR1^{CreER/+}$) mice. White and orange arrows indicated c-fos + cells were enlarged at the bottom-left of the middle and right panels to show the co-labeling with Npr1 and Sst, respectively. (b, c) Statistic data showed that C48/80 induced increase of overall c-fos + cell number in WT mice were greatly reduced in the microglia ablation mice (b, $p < .0001$ for both naïve vs. WT + C48/80 and WT + C48/80 vs. ablation + C48/80), and increase of c-fos + percentage of Npr1+ and Sst + neurons were also significantly reduced (c, $p < .0001$ for naïve vs. WT + C48/80 in Npr1+ and $p = .0263$ in Sst + cells, $p = .00213$ for WT + C48/80 vs. ablation + C48/80 in Npr1+ cells, $p = .00040$ for WT + C48/80 vs. ablation + C48/80 in Sst + cells). $n = 13$ and 15 images for WT + C48/80, and ablation + C48/80 group, respectively. Naïve data were equal to Figure 3. Samples were obtained from 3 mice for each group. * $p < .05$, ** $p < .01$, *** $p < .001$, **** $p < .0001$, un-paired t-test. Data were presented as mean \pm SEM.

P2Y12 KO mice with the HA, C48/80 and CQ models. As shown in Figure 6, the scratch responses to HA ($p = .891$), C48/80 ($p = .572$ for early and $p = .184$ for late stages) and CQ ($p = .352$ for early and $p = .865$ for late stages) treatment in the P2Y12 KO mice were all similar as that in the WT control mice, respectively. The results suggested that the P2Y12 receptors were not required for microglia to mediate the acute itch transmission.

The fractalkine or CX3CL1-CX3CR1 signal pathway is another well-known one to mediate the microglial-neuronal interaction and is involved in neuropathic pain and synaptic plasticity

(Paolicelli et al., 2011; Zhuang et al., 2007). We then tested the acute itch responses in the CX3CR1 KO mice with the HA, C48/80 and CQ models. The results in Figure 6 showed that the scratch responses to HA ($p < .0001$) in the CX3CR1 KO mice were significantly reduced compared to WT control, the responses to C48/80 were also significantly reduced in both early ($p = .0206$) and late ($p = .0012$) stages. However, the responses to CQ ($p = .1737$ for the early and $p = .8253$ for the late stages) were not altered and were comparable to the WT control in both stages. These results suggested that the CX3CL1-CX3CR1 signal

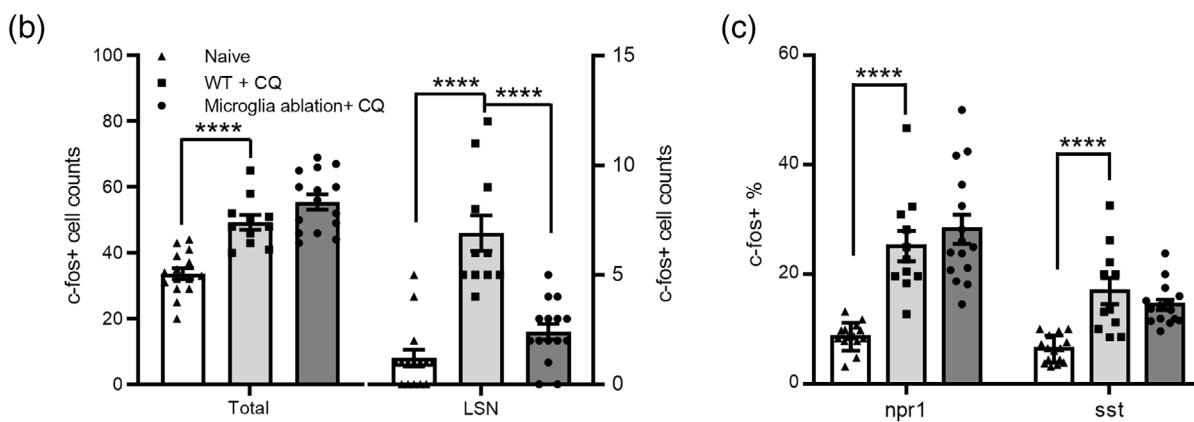
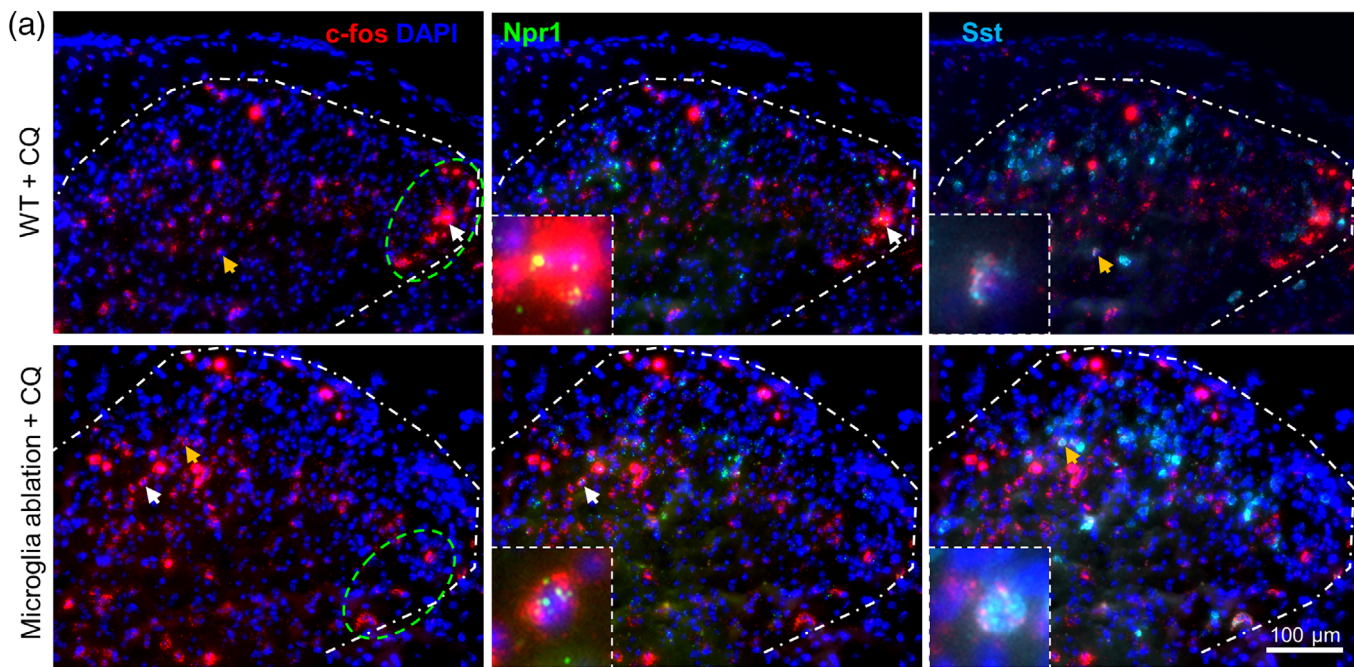


FIGURE 5 CQ-induced spinal c-fos mRNA expression was not reduced by microglia ablation. (A) representative RNAscope images showed triple labeling of c-fos, Npr1 and Sst mRNA in the spinal dorsal horn of CQ treated WT and microglia ablation ($ROSA^{IDTR};CX3CR1^{CreER/+}$) mice. White and orange arrows indicated c-fos + cells were enlarged at the bottom-left of the middle and right panels to show the co-labeling with npr-1 and Sst, respectively. (b, c) Statistic data showed that CQ induced increase of overall c-fos + cell number in WT mice were remained in the microglia ablation mice (b, $p < .0001$ for naïve vs. WT + CQ, $p = .0732$ for WT + CQ vs. ablation + CQ), but the c-fos + cells in the LSN within the green circle indicated area were reduced ($p < .0001$). The increase of c-fos + percentage of Npr1+ and Sst + neurons were also remained (c, $p < .0001$ for naïve vs. WT + CQ in both Npr1+ and Sst + cells, $p = .439$ for WT + CQ vs. ablation + CQ in Npr1+ cells, $p = .296$ for WT + CQ vs. ablation + CQ in Sst + cells). $n = 11$ and 15 images for WT + CQ, and ablation + CQ group, respectively. Naïve data were equal to Figure 3. Samples were obtained from three mice for each group. **** $p < .0001$, un-paired t -test. Data were presented as mean \pm SEM.

pathway was required for microglial activation to mediate the HA-dependent itch transmission, but this pathway is not necessary for CQ-induced itch responses.

To confirm that the spinal level of microglia anticipated in the acute itch transmission, we examined the effects of intrathecal administration of microglia inhibitor, minocycline, and CX3CR1 antagonist, JMS-17-2 on acute itch transmissions. With minocycline ($50 \mu\text{g}$ in $5 \mu\text{L}$ ACSF, i.t.) treatment at 30 min prior to the itch agent applications, the scratch responses to both C48/80 and CQ were significantly reduced in the late stage ($p = .0039$ for C48/80, $p = .0007$

for CQ), but not in the early stage ($p = .219$ for C48/80, $p = .282$ for CQ) comparing with vehicle controls. Moreover, we compared the effects of minocycline between male and female mice. The responses to both C48/80 and CQ were all in a similar level between the two sex groups, with or without minocycline treatment (Figure S6). Therefore, microglia activation mediated itch transmission was not sex dependent. With JMS-17-2 ($10 \mu\text{M}$ in ACSF, $5 \mu\text{L}$, i.t.) treatment at 30 min prior to the itch agent applications, the scratch responses to C48/80 were significantly reduced in the late stage ($p = .0152$), but not early stage ($p = .453$); the scratch responses to CQ were

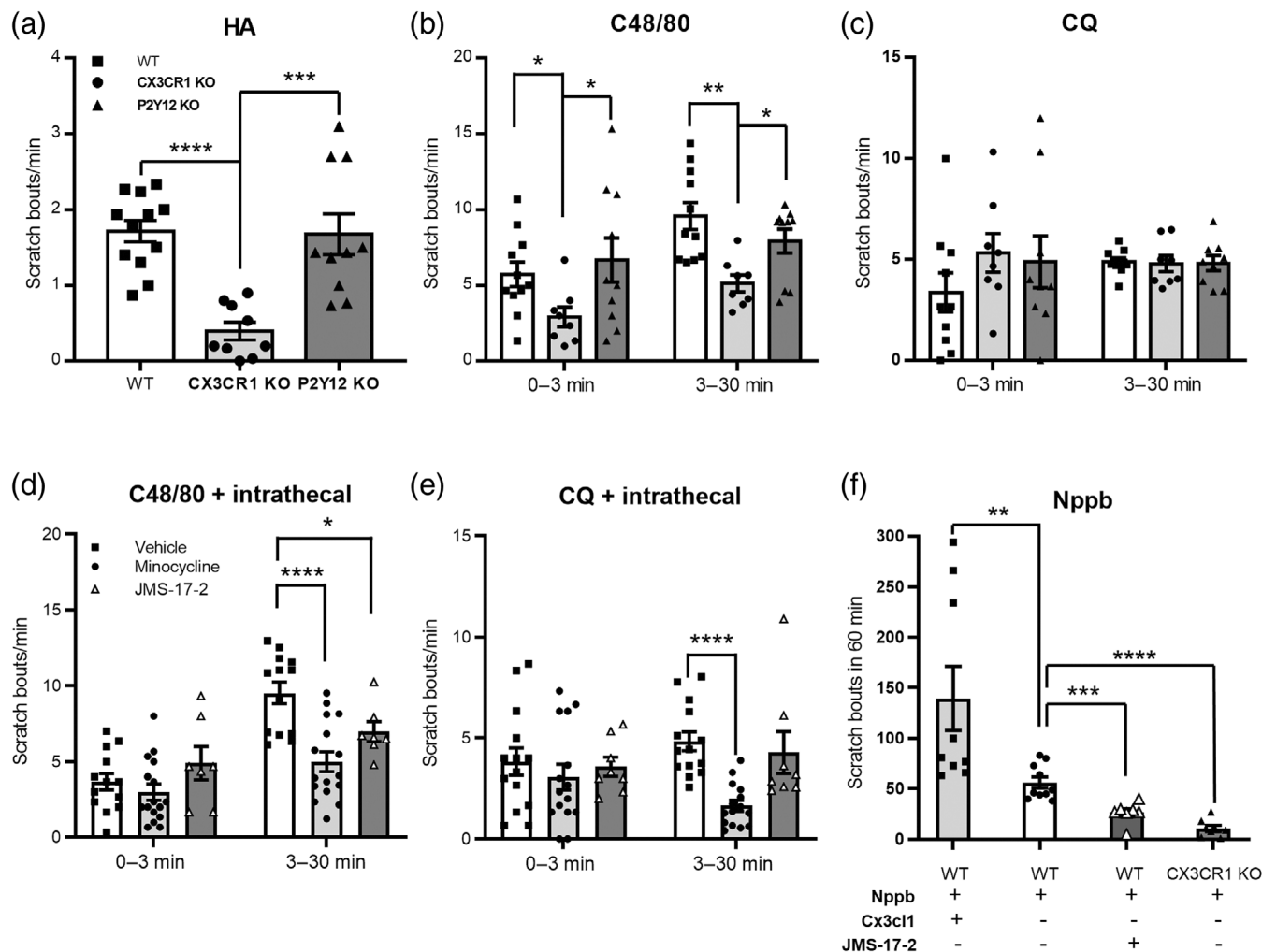


FIGURE 6 CX3CR1, but not P2Y12 receptor deficit impaired histamine dependent itch responses. (a) The scratch responses to HA in the CX3CR1 KO mice were significantly less than in the WT and P2Y12 KO mice during the 30 min observation ($n = 12, 9$ and 10 for WT, CX3CR1 KO and P2Y12 KO group, respectively; $p < .0001$ for WT vs. CX3CR1 KO, $p = .891$ for WT vs. P2Y12 KO). (b) The scratch responses to C48/80 in the CX3CR1 KO mice were significantly less than in the WT and P2Y12 KO mice at both the early ($p = .0206$ for WT vs. CX3CR1 KO, $p = .572$ for WT vs. P2Y12 KO) and late ($p = .0012$ for WT vs. CX3CR1 KO, $p = .184$ for WT vs. P2Y12 KO) stages ($n = 11, 8$ and 10 for WT, CX3CR1 KO and P2Y12 KO group, respectively). (c) The Scratch responses to CQ in both the CX3CR1 KO and P2Y12 KO mice were similar as in WT mice at both the early ($p = .174$ for WT vs. CX3CR1 KO, $p = .352$ for WT vs. P2Y12 KO) and late ($p = .825$ for WT vs. CX3CR1 KO, $p = .865$ for WT vs. P2Y12 KO) stages ($n = 10, 8$ and 9 for WT, CX3CR1 KO and P2Y12 KO group, respectively). (d) Intrathecal injection of microglia inhibitor, minocycline ($50 \mu\text{g}$ in $5 \mu\text{L}$ ACSF) or CX3CR1 antagonist, JMS-17-2 ($10 \mu\text{M}$ in ACSF, $5 \mu\text{L}$) to WT mice significantly reduced the late-stage scratch responses to C48/80 ($n = 13$ for vehicle, $n = 16$ for minocycline, $n = 7$ for JMS-17-2; $p < .0001$ for minocycline vs. vehicle, $p = .0319$ for JMS-17-2 vs. vehicle). (e) Intrathecal injection of microglia inhibitor, minocycline ($50 \mu\text{g}$ in $5 \mu\text{L}$ ACSF), but not CX3CR1 antagonist, JMS-17-2 ($10 \mu\text{M}$ in ACSF, $5 \mu\text{L}$) to WT mice significantly reduced the late-stage scratch responses to CQ ($n = 14$ for vehicle, $n = 15$ for minocycline, $n = 8$ for JMS-17-2; $p < .0001$ for minocycline vs. vehicle, $p = .581$ for JMS-17-2 vs. vehicle). (f) Direct intrathecal Nppb ($10 \mu\text{g}$ in $5 \mu\text{L}$ ACSF) injection induced scratch responses in WT mice were enhanced by CX3CL1 ($0.3\text{--}0.4 \mu\text{g}$ in $5 \mu\text{L}$ ACSF) co-injection ($p = .0061$, $n = 10$ for Nppb, $n = 9$ for nppb+CX3CL1), and were reduced by CX3CR1 inhibitor JMS-17-2 ($10 \mu\text{M}$) co-injection ($p = .0010$, $n = 7$), while Nppb injection induced scratch responses in CX3CR1 KO mice ($n = 8$) were dramatically less than in WT mice ($p < .0001$). * $p < .05$, ** $p < .01$, *** $p < .001$, **** $p < .0001$, un-paired t -test. Data were presented as mean \pm SEM.

not altered in any stage ($p = .076$ for the early stage, $p = .873$ for the late stage) comparing with vehicle controls (Figure 6d,e). The results confirmed that spinal microglia were involved in the late-stage itch transmission of both the HA-dependent and non-dependent (CQ) types, and spinal microglial CX3CR1 pathway was recruited to the HA-dependent itch transmission, but not CQ-induced itch transmission.

To further study how the CX3CL1-CX3CR1 signal pathway affects the HA itch neuronal circuits. We examined the spinal c-fos activation with RNAscope again in the CX3CR1 KO mice that treated with HA, C48/80 and CQ, respectively, and co-labeled the Npr1 and Sst neurons. As shown in Figure 7a-f and Figure S7, the total c-fos + cells in the spinal dorsal horn of HA ($p < .0001$) or C48/80 ($p < .0001$) treated CX3CR1 KO mice were

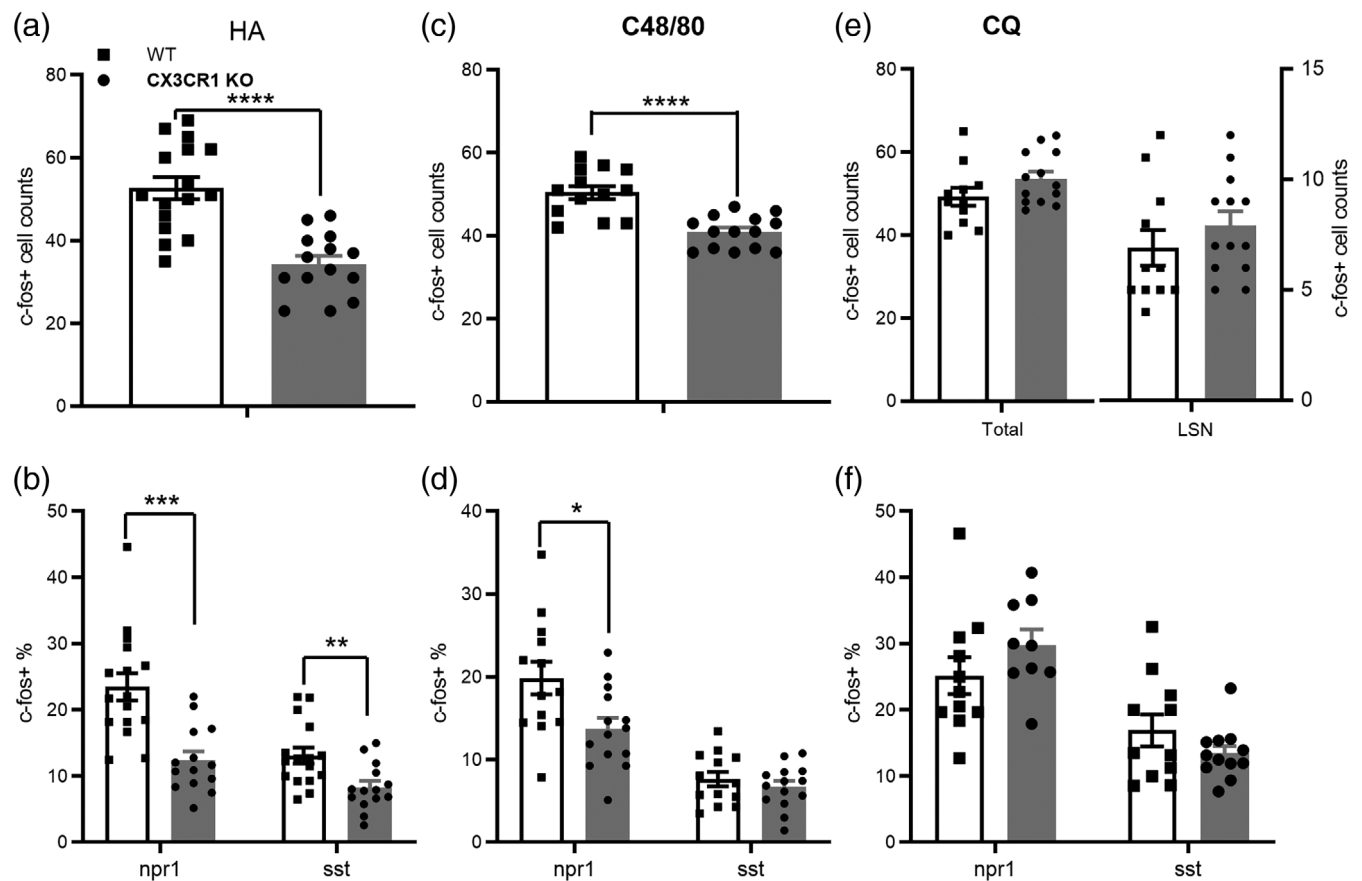


FIGURE 7 Histamine dependent spinal Npr1 neuronal activity required CX3CL1-CX3CR1 microglial co-activation. (a, b) HA-induced increase of overall c-fos + cell number in WT mice were greatly reduced in the CX3CR1 KO mice ($p < .0001$), and the increase of c-fos + percentage of Npr1+ ($p = .00014$) and Sst + ($p = .0049$) cells were also significantly reduced ($n = 16$ for WT, $n = 14$ for CX3CR1 KO). (c, d) C48/80 induced increase of overall c-fos + cell number in WT mice were greatly reduced in the CX3CR1 KO mice ($p < .0001$), and the increase of c-fos + percentage of Npr1+ ($p = .0143$), but not Sst + ($p = .419$) cells were also significantly reduced ($n = 13$ for WT, $n = 14$ for CX3CR1 KO). (e, f) CQ induced increase of overall ($p = .137$) and LSN ($p = .3265$) c-fos + cell number in WT mice were remained in the CX3CR1 KO mice, and the increase of c-fos + percentage of Npr1+ ($p = .117$) and Sst + ($p = .155$) cells were also remained ($n = 11$ for WT, $n = 13$ for CX3CR1 KO). Samples were obtained from three mice for each group. * $p < .05$, *** $p < .001$, **** $p < .0001$, un-paired t-test. Data were presented as mean \pm SEM.

significantly decreased compared with the WT control mice that received HA and C48/80 treatment, respectively. Consistent with the behavior data, the CQ-induced total ($p = .1367$) and LSN ($p = .3265$) c-fos expression in CX3CR1 KO mice was comparable to the WT control that received CQ treatment. For the Npr1+ neurons, the percentage of c-fos + cells in HA ($p = .00014$) and C48/80 ($p = .0143$) treated CX3CR1 KO mice were both significantly less than that of the WT control models, respectively; while the percentage of c-fos + cells in CQ treated CX3CR1 KO mice were comparable to WT control model ($p = .1169$). For the Sst + neurons, the percentage of c-fos + cells in HA ($p = .0049$) treated CX3CR1 KO mice were significantly less than that of the WT control model, but C48/80 ($p = .4188$) induced c-fos+/Sst + neurons were not significantly reduced. The CQ ($p = .1552$) induced c-fos+/Sst + neurons were not affected by CX3CR1 KO. These results suggested that the CX3CL1-CX3CR1 microglial signal pathway played a critical role to promote the primary neuronal responses to HA-dependent itch signals in the spinal level, particularly for the Npr1+ neurons.

To dissect whether microglia regulated the Npr1+ neuronal activities through modulating the afferent neural transmitter release from DRG or through modulating the Npr1+ neuronal excitability. We did intrathecal Nppb injection to directly activate the spinal Npr1+ neurons, with which the afferent input was bypassed. The Nppb injection (10 μ g in 5 μ L ACSF) induced scratch responses in WT mice as expected. With CX3CL1 (0.3–0.4 μ g in 5 μ L) co-injection, the responses were significantly increased ($p = .0061$). With the CX3CR1 antagonist JMS-17-2 (10 μ M) co-injection, the responses were significantly decreased ($p = .0010$). And the Nppb induced scratch responses in the CX3CR1 KO mice were dramatically less than that in the WT mice ($p < .0001$) (Figure 6f). These results together with the c-fos data suggested that microglia regulated HA-dependent itch transmission by enhancing the Npr1+ neuronal responses to Nppb, which was dependent on the CX3CL1-CX3CR1 pathway.

To investigate where did the CX3CL1 signal come from, we examined the Cx3cl1 mRNA expression in spinal cord and DRG. The Cx3cl1 mRNA was also constantly expressed in the spinal dorsal horn

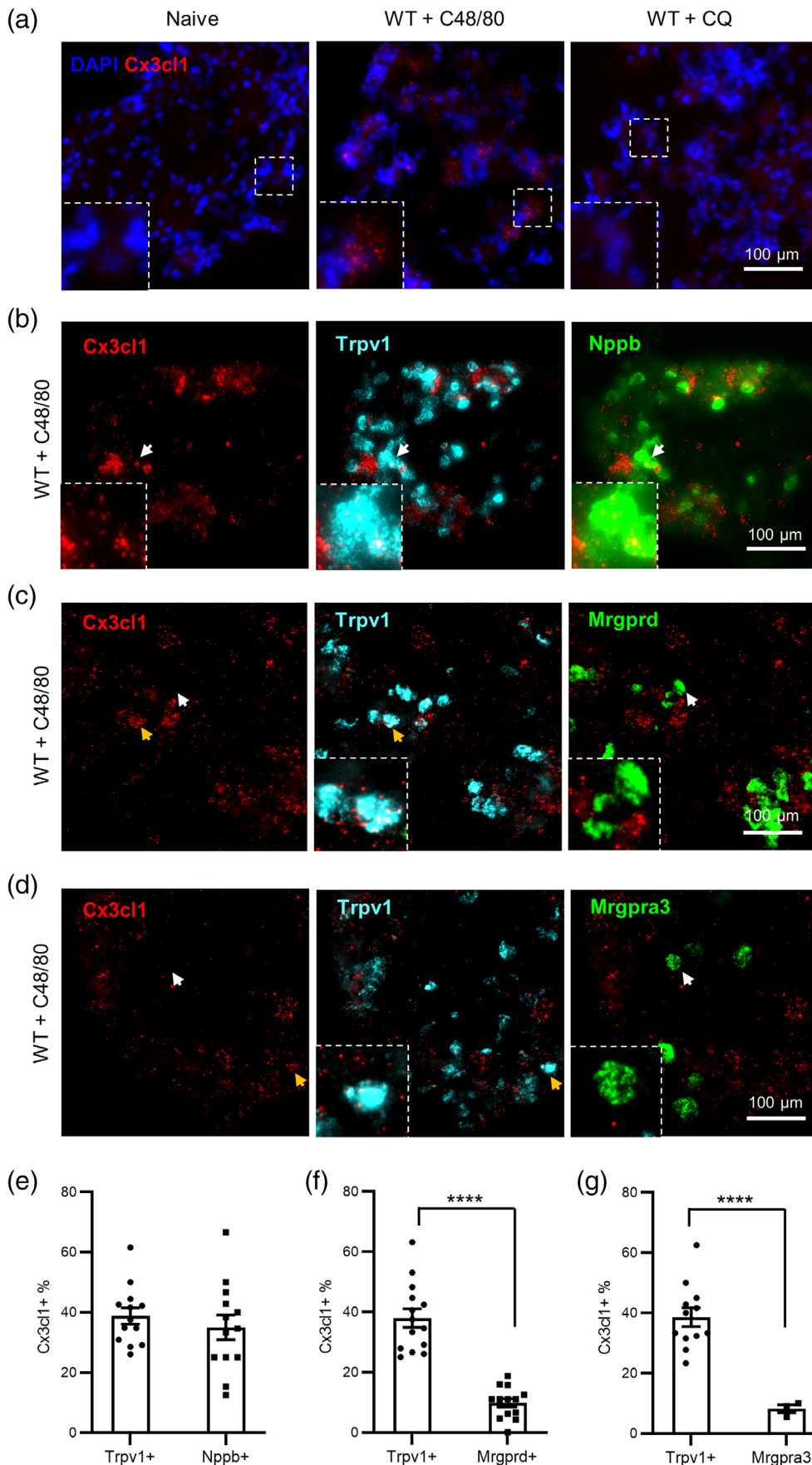


FIGURE 8 C48/80, but not CQ-induced *Cx3cl1* upregulation in DRG Neurons.

(a) Representative RNAscope images showed *Cx3cl1* mRNA expression in the DRG. *Cx3cl1* mRNA was not detectable in the DRG of naive ($n = 10$ image samples) WT mice nor CQ ($n = 14$ image samples) treated (90 min post CQ) WT mice, but was seen in the DRG of C48/80 treated (90 min post C48/80) WT mice ($n = 11$ of 14 image samples). (b) *Cx3cl1*, *Trpv1* and *Nppb* triple RNAscope assay indicated *Cx3cl1* mRNA expression was partially overlapped with *Trpv1* and *Nppb*, and all *Nppb*⁺ cells were *Trpv1*⁺. (c) *Cx3cl1*, *Trpv1* and *Mrgprd* triple RNAscope assay indicated *Cx3cl1* mRNA expression in *Trpv1*⁺ neurons, but not in *mrgprd*⁺ neurons. (d) *Cx3cl1*, *Trpv1* and *Mrgpra3* triple RNAscope assay indicated *Cx3cl1* mRNA expression in *Trpv1*⁺ neurons, but not in *Mrgpra3*⁺ neurons. (e–g) Statistical data showed similar percentage of *Nppb*⁺ and *Trpv1*⁺ neurons (E, $n = 13$ images, $p = .371$), but significantly less percentage of *Mrgprd*⁺ (E, $n = 14$ images) and *Mrgpra3*⁺ (F, $n = 12$ images) neurons were *Cx3cl1* positive, respectively. Samples were obtained from three mice for each group. **** $p < .0001$, paired *t*-test. Data were presented as mean \pm SEM.

in naïve WT mice but was hard to detect any change at 90 min after the itch agent applications (Figure S9). However, the Cx3cl1 mRNA was almost non-detectable in naïve DRG with the same RNAscope protocol. After CQ treatment (90 min), the mRNA signal was still non-detectable in the DRG. After C48/80 treatment (90 min), the Cx3cl1 mRNA expression was clearly seen in DRG (Figure 8a). To examine in what type of cells the Cx3cl1 was upregulated by C48/80 stimuli, we did Triple staining with Trpv1 and one of the three type of itch related neuron markers, Nppb, Mrgpra3 and Mrgprd, respectively. As shown in Figure 8b–g, around 38% of Trpv1+ cells were Cx3cl1+. The Nppb+ NP3 cells were all Trpv1+ and showed a similar Cx3cl1+ percentage (Figure 8e, S10). However, Cx3cl1 was shown in less than 10% of either the Mrgprd+ (NP1, responsible for β -alanine) or Mrgpra3+ (NP2, responsible for CQ) neurons, both were dramatically less than in the Trpv1+ neurons (Figure 8c,d,f,g). The results suggested that the HA-activated DRG sensory neurons could be one of the sources of CX3CL1, and CX3CL1 could be co-released with Nppb at the terminal projecting to spinal dorsal horn. However, the spinal local source of CX3CL1 seemed also contribute to the enhancement of Nppb signal effects, since CX3CR1 inhibition or KO reduced the direct Nppb stimuli-induced itch responses.

3 | DISCUSSION

3.1 | The neuronal circuit differences for HA and CQ elicited itch signal transmission

The HA and CQ-triggered itch signal processing pathways share some common parts in both peripheral DRG and central spinal cord. The CQ receptor, Mrgpra3 expressing DRG neurons also express HA receptors and are required for HA itch transmission (Han et al., 2013); NPRA and SST expressing interneurons in spinal cord are required for both HA and CQ signal processing (Fatima et al., 2019). However, the pathway differences are critical to define these two types of chemical itch. HA acts directly on H1 and H4 receptors and requires the activation of TRPV1 channels (Imamachi et al., 2009). However, DRG neuronal excitation triggered by CQ requires TRPA1, instead of TRPV1 (Wilson et al., 2011). The different activation mechanisms are likely to trigger different neural transmitters release to the spinal cord. For example, glutamate transmission from Mrgpra3+ DRG neurons is required for both CQ and HA-elicited itch, but NMB from Mrgpra3+ DRG neurons is only required for CQ-elicited itch (Cui et al., 2022). On the other hand, although NPRA neurons contribute to CQ signal relay, but it is not dependent on the Nppb-NPRA pathway that Npr1 KO did not affect CQ-induced itch responses (Liu et al., 2020). The signal molecular for NPRA neurons to relay CQ-induced activity is still unknown. Therefore, it is possible that there are some un-discovered neural transmitters responsible for certain kinds of itch signal transmission. Here we showed that the CX3CL1 signal was required for HA-dependent itch signal transmission. It is

quite possible that CX3CL1 was used as one of the neural transmitters by the DRG neurons to trigger the HA-dependent itch transmission.

3.2 | The CX3CL1 release mechanism triggered by HA stimulus

The CX3CL1-CX3CR1 pathway was previously reported to be involved in microglial promotion of neuropathic pain (Zhuang et al., 2007). CX3CL1 is expressed in both DRG and spinal cord. Peripheral nerve injury was thought to cause the CX3CL1 cleavage and release from DRG neurons (Verge et al., 2004; Zhuang et al., 2007). Here we observed an obvious upregulation of Cx3cl1 mRNA in the DRGs with C48/80 stimulus. C48/80 triggered endogenous HA release through mast cell degranulation. However, mast cell degranulation not only releases histamine, but also releases other cytokines and chemokines, which also induced neutrophil infiltration in turn. These factors cause tissue edema and inflammatory pain (Abraham & St John, 2010; Chatterjea et al., 2012). The pain pathway activation may trigger Cx3cl1 expression in DRG neurons other than the itch related Nppb+ cells. That could explain the Cx3cl1 signals seen in Trpv1- cells. Moreover, the higher percentage of Cx3cr1+ signals in Nppb+ than in Mrgpra3+ or Mrgprd+ cells suggested that DRG Cx3cl1 upregulation was neuronal activity dependent. On the contrary, CQ stimulus did not change the Cx3cl1 mRNA expression. The difference in DRG Cx3cl1 upregulation was correlated with the involvement of CX3CR1 receptors for the itch behavioral responses. Taken together, our results suggested that the HA dependent and non-dependent itch pathways had distinguished downstream responses even at DRG level.

Where was the fractalkine released is still a question remained to be resolved. Central microglia were most likely the major signal receiver of fractalkine, because the reduction of c-fos in spinal Npr1 and Sst neurons and the inhibition of itch responses to HA or C48/80 were seen in both the microglia ablation and CX3CR1 KO mice. The requirement of CX3CR1 activation for intrathecal Nppb induced itch responses further proved this point. However, the peripheral macrophages could also contribute to the enhancement of HA-dependent itch signal transmission by responding to fractalkine. In the CSF1R strategy ablation mice or the CX3CR1 KO mice, we observed the inhibition of behavioral response to C48/80 in very early stage (0–3 min), but this phenomenon was not seen in the two kinds of iDTR strategy ablation mice, in which the peripheral macrophages were partially or fully remained. The DRG macrophages are surrounding the neuron bodies and could respond quickly to the fractalkine signal that released from the DRG neuron bodies. The signal added on central microglia could come from the DRG release diffusing to CSF or directly released from DRG projecting terminals. On the other hand, since Cx3cl1 was highly expressed in spinal dorsal horn, the spinal neuronal activities could also trigger fractalkine release.

3.3 | Microglial pathways for chemical itch other than CX3CL1-CX3CR1

CQ elicited itch response did not require the CX3CL1-CX3CR1 pathway, but microglia depletion still strongly inhibited the behavioral responses. Although the percentage of *c-fos* mRNA upregulated Npr1 and Sst neurons were not decreased in the CQ treated microglia depletion mice, we did see an overall *c-Fos* protein level decrease in spinal dorsal horn with immunostaining (Figure S6) and *c-fos* mRNA decrease in the LSN. The different results between mRNA and protein assays could be due to the different technique sensitivities of RNA-scope and immunostaining that RNA-scope was more sensitive and would detect and amplify weak *c-fos* signals. These results suggested that microglia also contributed to the CQ elicited itch signal transmission at spinal level and there were some other signals that triggered microglial responses. For neuropathic pain, the purinergic signal was thought to be important to activate microglia and promote the development of chronic pain. Depletion the purinergic receptors, such as P2X4 (Tsuda et al., 2009), P2X7 (Chessell et al., 2005) or P2Y12 (Tozaki-Saitoh et al., 2008), all dramatically alleviated or totally blocked neuropathic pain. P2X4 can respond to ATP at nanomolar level, which is about one thousand times lower than that for P2X7. Therefore, P2X4 could be a good candidate to mediate the quick microglial responses for itch transmission. P2Y12 receptors are highly expressed in central microglia and mediate the microglial process movement toward ATP gradient (Haynes et al., 2006). Unexpectedly, our results showed that the P2Y12 KO mice did not show any deficits in chemical itch response, suggesting that this directional process movement was not necessary for microglia to enhance neuronal excitability quickly. Further studies are required to examine other signal pathways for microglia to promote chemical itch transmission.

The down-stream of microglial responses to itch signals is another question remained to be resolved in the future. Cytokines such as IL-31 and TNF- α have been found to contribute to acute and chronic itch (Cevikbas et al., 2014; Miao et al., 2018). Microglia was one of the major sources of TNF- α and are involved in acute inflammatory pain by enhancing neuronal excitability (Berta et al., 2014). Thus, microglia released TNF- α is a potential mediator for acute chemical itch as well. BDNF is known to be the down-stream of P2X4 that released by microglia to mediate neuropathic pain through disinhibiting mechanism (Beggs et al., 2012). Whether this pathway also contributes to itch signal transmission is worthy to test as well.

The different requirement of CX3CL1-CX3CR1 pathway for HA-dependent and non-dependent itch transmission suggested that the microglial response to the two kinds of itch circuits could be different. Nppb-NPRA pathway seemed required microglial co-activation to trigger the Npr1 neuron responses. On the contrary, Npr1 neuron response to CQ signal need neither Nppb nor CX3CL1-induced microglial activation.

In conclusion, our present study revealed that central microglia played a critical role in promoting acute chemical itch signal transmission that induced by HA dependent or non-dependent (CQ) agents. However, microglia participated in the HA dependent and non-dependent itch signal transmission in different ways. For the HA

dependent signals, the CX3CL1-CX3CR1 signal pathway could be the major component to trigger microglial responses and then promote the neuronal activities of the spinal Npr1+ and Sst + neurons. The CX3CL1 signal was most likely to be released by the HA-activated DRG sensory neurons that projected to spinal dorsal horn. However, how the CQ signal activate microglia and the downstream microglial response mechanisms remained unresolved.

4 | MATERIALS AND METHODS

4.1 | Animals

All experimental procedures were approved by the Institutional Animal Care and Use Committee of Nanchang University. We followed the guidelines set forth by the Guide of the Care and Use of Laboratory Animals 8th Edition. The P2Y12 KO mice were originally obtained from Dr. Long-Jun Wu lab at Mayo Clinic, which was originally generated by Dr. Pamela B. Conley (André et al., 2003). CX3CR1-CreER (#021160), TMEM119-CreER (#031820), TMEM119-EGFP (#031823), CSF1R-flox (#021212), and ROS26-iDTR (007900) mice were originally purchased from Jackson Laboratory. CX3CR1-CreER mice were crossed with CSF1R-flox mice to get the CSF1R^{flox/flox};CX3CR1^{CreER/+} mice, and crossed with the ROSA-iDTR mice to get the ROSA^{iDTR/+};CX3CR1^{CreER/+} mice. TMEM119-CreER mice were crossed with the ROSA-iDTR mice to get the ROSA^{iDTR/+};TMEM119^{CreER/+} mice. Wild type (WT) C57BL6/J mice were obtained from SLAC laboratory animal CO. LTD (Changsha, China). Mice were group (4–5 per cage) housed in 12/12 light/dark cycle, 23 \pm 1°C vivarium environment. Food and water were available ad libitum. Mice (8–14 weeks old) were assigned to experimental groups randomly within a litter. Experimenters were blind to drug treatments and mouse genotypes until all data collection was done. Both male and female mice were used.

4.2 | Microglia ablation

4.2.1 | CSF1R strategy

CSF1R^{flox/flox};CX3CR1^{CreER/+} transgenic mice were used for this purpose. Intraperitoneally (i.p.) injection of tamoxifen (TM, 150 mg/kg in corn oil, three doses with 48-h intervals) were used to trigger the *csf1r* gene knockout in CX3CR1+ cells. CSF1R^{flox/flox} mice were used as control and received the same doses of TM. Acute itch models were tested at 24 h after the last TM treatment.

4.2.2 | iDTR strategies

ROSA^{iDTR/+};CX3CR1^{CreER/+} and ROSA^{iDTR/+};TMEM119^{CreER/+} transgenic mice were used. For the ROSA^{iDTR/+};CX3CR1^{CreER/+} mice, four

doses of TM (150 mg/kg in corn oil) were i.p. injected with 48-h intervals to trigger the DTR expression in CX3CR1⁺ cells. Three weeks after the last TM injection, two doses of diphtheria toxin (DT) were i.p. injected (0.75 µg per mice) with a 48-h interval to ablate central microglia but avoided to ablate most of the circulating monocytes and peripheral macrophages. For the ROSA^{IDTR/+}; TMEM119^{CreER/+} mice, 10 doses of TM (150 mg/kg in corn oil) were i.p. injected with 24-h intervals to trigger the DTR expression in central microglia. Five days after the last TM injection, two doses DT were i.p. injected (0.75 µg per mice) with a 48-h interval to ablate central microglia.

4.3 | Intrathecal injections

The microglia activation inhibitor, minocycline (10 µg/µL in ACSF that contained 0.1% DMSO and 0.4% PEG300) and the CX3CR1 antagonist, JMS-17-2 (10 µM in ACSF that contained 0.1% DMSO and 0.4% PEG300) were intrathecal (i.t.) injected as previously described. In brief, mice were hand restricted, a 31G needle that attached with 10-µL Hamilton syringe (Hamilton Bonaduz AG) were direct lumbar punched between L5 and L6 vertebrae of the spine with around 15° angle, successful insertion was indicated by tail flick. For Nppb injection, the injecting site was between L4 and L5. 5 µL of the drug solution or control vehicle was injected into the spinal fluid space in 2 min, and the needle was held in place for one more minute. The i.t. injections were done 30 min prior to the itch agent application.

4.4 | Behavioral testing

4.4.1 | Acute mechanical itch

To test the acute mechanical itch, the fur behind the ears was shaved 5 days before testing. Mice were habituated for 30 min in behavioral testing apparatus (IITC, Life Science) for two consecutive days. On the testing day, mice were placed in the plastic chambers and allowed at least 30 min for habituation. Mice then received five separate mechanical stimuli for 1 s with 3–5 s intervals at randomly selected sites on the skin behind the ears. Mechanical stimuli were delivered with von Frey filaments (0.02–0.16 g, North Coast medical). The scratching response of hind paw toward the poking site was considered as a positive response (Pan et al., 2019).

4.4.2 | Acute chemical itch

To test the acute chemical itch, the fur on the neck was shaved 5 days before testing. Mice were habituated the same as for the acute mechanical itch test. On the testing day, mice were placed in the plastic chambers and allowed at least 30 min for habituation. Then the

behavior of mice was video recorded for at least 30 min after chemical injection. Compound histamine (50 µg, Sigma #H7250) in 10 µL of sterile saline was injected intradermally into the nape. Compound chloroquine (200 µg, Sigma #C6628), β-alanine (50 mM Sigma #146064), C48/80 (100 µg, Sigma #C2313) in 50 µL of sterile saline was injected intradermally into the nape. Scratching bouts were counted for 30 min after injection.

To observe the intrathecal nppb (10 µg in 5 µL ACSF) injection-induced itch behavior, the mice were put into the chambers immediately after the injection, and the behaviors were video recorded for 60 min.

4.4.3 | Dry skin-induced chronic itch

The mouse hair of the nape was shaved 2 days before treatment. Dry skin was induced by application of 1 mL 1:1 mixture of acetone and diethyl ether for 10 min, followed by water for 30 s (AEW). The mice were treated with AEW twice daily (morning and evening) for 8 days (Jing et al., 2018). On the second, fourth, sixth, eighth day, at 2 h post the first daily AEW, the spontaneous scratching behavior was recorded for 1 h after a 60 min habituation session. For microglia depletion, the tamoxifen pre-treated (3 weeks) mice were given DT injection (0.75) at day 4 and day 6 after the behavior recording. Both the microglia depletion (CX3CR1^{CreER/+}; ROSA^{IDTR/+}) and control (ROSA^{IDTR/+}) mice received the same treatment of tamoxifen and DT.

4.5 | Immunofluorescence

Experimental mice were deeply anesthetized by 1% pentobarbital sodium (50 mg/kg, i.p.) and transcardially perfused with 0.9% saline followed by 4% paraformaldehyde solution. The cervical segment of spinal cord (C3–C5) and their connected DRGs were collected and post-fixed with the same 4% PFA for 4–6 h at 4°C, and then gradient dehydrated in 20% and 30% (wt/vol) sucrose solution sequentially. Sample sections (14 µm in thickness) were prepared on gelatin-coated glass slide with a freezing microtome (Leica CM900, Germany). The sections were blocked with 5% goat serum and 0.3% Triton X-100 (Sigma) in TBS buffer for 45 min, and then incubated overnight at 4°C with primary antibody for rabbit-anti-Iba1 (1:1000, Abcam, Catalogue ab178846), rat-anti-F4/80 (1:500, Biolegend, Catalogue #123102), rabbit-anti-CX3CL1 (1:500, NOVUS, Catalogue NBP1-49539) and rabbit-anti-c-Fos (1:500, Cell Signaling, Catalogue #2250). After rinse three times for at least 30 min with TBS buffer, the sections were then incubated for 90 min at room temperature with secondary antibodies (1:500, Alexa Fluor 568, Alexa Fluor 488, Life Technologies). After three rinses, slices were incubated with DAPI solution for 5 min and followed by washout. Fluorescent images were obtained with a fluorescence microscope (EVOS FL Color, life technologies). Cell counting and fluorescent signal intensity were quantified using ImageJ software (1.52a, National Institutes of Health, Bethesda, MD).



4.6 | RNAscope

The frozen section samples of the same sets for the above immunofluorescence were taken. Samples were washed in PBS for 5 min and air dried. Next about 5–8 drops of RNAscope® hydrogen peroxide were added to coat the samples and incubated at room temperature for 10 min and then washed with distilled water. Then immerse the samples into the RNAscope target repair reagent at 98–100°C for 5 min, then transferred to distilled water for cooling. The samples were then incubated with 100% ethanol for 3 min and drawn a hydrophobic ring around it. Appropriate amount of RNAscope® protease III reagent was dropped to completely cover the sections, and incubation was conducted at 40°C for 30 min. The samples were then processed immediately with the provided standard RNAscope assay (Advanced Cell Diagnostics, Inc.). mm-fos, mm-npr1 and mm-sst probes were used for triple labeling at opal 690, 520 and 570 channels. mm-cx3cl1 probe was used for single labeling at opal 690 channel. The samples were finally stained with DAPI. The fluorescent images were obtained with the EVOS microscope at $\times 20$ and analyzed with ImageJ as well. For each mouse, 3–6 sections were chosen that preferred to intact spinal dorsal horn or DRG and without sectioning artifact. The signal threshold for a given channel was set based on sections of the negative probe control. Positive cell threshold was defined as a signal cluster with three dots or an area covered more than three dots within a DAPI-defined area.

4.7 | Statistical analysis

Statistical analysis was performed using GraphPad Prism 7.00 (GraphPad software, Inc.). Unpaired Student's test (*t*-test) and two-way ANOVA with repeated measurement were applied for group-group comparison. $p < .05$ was considered statistically significant.

AUTHOR CONTRIBUTIONS

Jiyun Peng, Haili Pan and Yuxiu Yang conceived of the study. Yuxiu Yang, Bin Mou, Qi-Ruo Zhang, Jian-Yun Xhang, Hong-Xue Zhao, Xiao Yun, Ming-Tao Xiong and Ying Liu performed experiments and analyzed data. Jiyun Peng, Yuxiu Yang, Yong U. Liu, Haili Pan, Chao-Lin Ma and Bao-Ming Li wrote the manuscript.

ACKNOWLEDGMENTS

This work was supported by the Jiangxi Province “2000 talent plan” to Jiyun Peng (jxsq2018106039), the National Natural Science Foundation of China (32060199 to Jiyun Peng, 82071245 to Haili Pan, and 31971035, 31771182 to Bao-Ming Li) and Jiangxi Province Natural Science Foundation (20224ACB206016 to Jiyun Peng, 20171ACB20002 to Bao-Ming Li).

CONFLICT OF INTEREST STATEMENT

The authors declare no competing interests.

DATA AVAILABILITY STATEMENT

The source data for all figures were provided as a supporting document. Detailed raw data are available from the corresponding author upon request.

ORCID

Jiyun Peng  <https://orcid.org/0000-0002-7410-131X>

REFERENCES

- Abraham, S. N., & St John, A. L. (2010). Mast cell-orchestrated immunity to pathogens. *Nature Reviews. Immunology*, 10(6), 440–452. <https://doi.org/10.1038/nri2782>
- Akiyama, T., Tominaga, M., Takamori, K., Carstens, M. I., & Carstens, E. (2014). Roles of glutamate, substance P, and gastrin-releasing peptide as spinal neurotransmitters of histaminergic and nonhistaminergic itch. *Pain*, 155(1), 80–92. <https://doi.org/10.1016/j.pain.2013.09.011>
- André, P., Delaney, S. M., LaRocca, T., Vincent, D., DeGuzman, F., Jurek, M., Koller, B., Phillips, D. R., & Conley, P. B. (2003). P2Y12 regulates platelet adhesion/activation, thrombus growth, and thrombus stability in injured arteries. *The Journal of Clinical Investigation*, 112(3), 398–406. <https://doi.org/10.1172/JCI17864>
- Beggs, S., Trang, T., & Salter, M. W. (2012). P2X4R+ microglia drive neuropathic pain. *Nature Neuroscience*, 15(8), 1068–1073. <https://doi.org/10.1038/nn.3155>
- Berta, T., Park, C. K., Xu, Z. Z., Xie, R. G., Liu, T., Lü, N., Liu, Y. C., & Ji, R. R. (2014). Extracellular caspase-6 drives murine inflammatory pain via microglial TNF- α secretion. *The Journal of Clinical Investigation*, 124(3), 1173–1186. <https://doi.org/10.1172/JCI72230>
- Brandt, E. B., & Sivaprasad, U. (2011). Th2 cytokines and atopic dermatitis. *Journal of Clinical and Cellular Immunology*, 2(3), 110. <https://doi.org/10.4172/2155-9899.1000110>
- Cevikbas, F., Wang, X., Akiyama, T., Kempkes, C., Savinko, T., Antal, A., Kukova, G., Buhl, T., Ikoma, A., Buddenkotte, J., Soumelis, V., Feld, M., Alenius, H., Dillon, S. R., Carstens, E., Homey, B., Basbaum, A., & Steinhoff, M. (2014). A sensory neuron-expressed IL-31 receptor mediates T helper cell-dependent itch: Involvement of TRPV1 and TRPA1. *The Journal of Allergy and Clinical Immunology*, 133(2), 448–460. <https://doi.org/10.1016/j.jaci.2013.10.048>
- Chatterjea, D., Wetzel, A., Mack, M., Engblom, C., Allen, J., Mora-Solano, C., Paredes, L., Balsells, E., & Martinov, T. (2012). Mast cell degranulation mediates compound 48/80-induced hyperalgesia in mice. *Biochemical and Biophysical Research Communications*, 425(2), 237–243. <https://doi.org/10.1016/j.bbrc.2012.07.074>
- Chen, X. J., & Sun, Y. G. (2020). Central circuit mechanisms of itch. *Nature Communications*, 11(1), 3052. <https://doi.org/10.1038/s41467-020-16859-5>
- Chessell, I. P., Hatcher, J. P., Bountra, C., Michel, A. D., Hughes, J. P., Green, P., Egerton, J., Murfin, M., Richardson, J., Peck, W. L., Grahames, C. B. A., Casula, M. A., Yiangou, Y., Birch, R., Anand, P., & Buell, G. N. (2005). Disruption of the P2X7 purinoceptor gene abolishes chronic inflammatory and neuropathic pain. *Pain*, 114(3), 386–396. <https://doi.org/10.1016/j.pain.2005.01.002>
- Cui, L., Guo, J., Cranfill, S. L., Gautam, M., Bhattacharai, J., Olson, W., Beattie, K., Challis, R. C., Wu, Q., Song, X., Raabe, T., Gradinaru, V., Ma, M., Liu, Q., & Luo, W. (2022). Glutamate in primary afferents is required for itch transmission. *Neuron*, 110(5), 809–823. <https://doi.org/10.1016/j.neuron.2021.12.007>
- Davidson, S., & Giesler, G. J. (2010). The multiple pathways for itch and their interactions with pain. *Trends in Neurosciences*, 33(12), 550–558. <https://doi.org/10.1016/j.tins.2010.09.002>
- Dong, X., & Dong, X. (2018). Peripheral and central mechanisms of itch. *Neuron*, 98(3), 482–494. <https://doi.org/10.1016/j.neuron.2018.03.023>
- Elmore, M. R., Najafi, A. R., Koike, M. A., Dagher, N. N., Spangenberg, E. E., Rice, R. A., Kitazawa, M., Matusow, B., Nguyen, H., West, B. L., & Green, K. N. (2014). Colony-stimulating factor 1 receptor signaling is necessary for microglia viability, unmasking a microglia progenitor cell in the adult brain. *Neuron*, 82(2), 380–397. <https://doi.org/10.1016/j.neuron.2014.02.040>
- Fatima, M., Ren, X., Pan, H., Slade, H. F. E., Asmar, A. J., Xiong, C. M., Shi, A., Xiong, A. E., Wang, L., & Duan, B. (2019). Spinal somatostatin-

- positive interneurons transmit chemical itch. *Pain*, 160(5), 1166–1174. <https://doi.org/10.1097/j.pain.0000000000001499>
- Gomez Perdiguero, E., Klapproth, K., Schulz, C., Busch, K., Azzoni, E., Crozet, L., Garner, H., Trouillet, C., de Bruijn, M. F., Geissmann, F., & Rodewald, H. R. (2015). Tissue-resident macrophages originate from yolk-sac-derived erythro-myeloid progenitors. *Nature*, 518(7540), 547–551. <https://doi.org/10.1038/nature13989>
- Han, L., Ma, C., Liu, Q., Weng, H. J., Cui, Y., Tang, Z., Kim, Y., Nie, H., Qu, L., Patel, K. N., Li, Z., McNeil, B., He, S., Guan, Y., Xiao, B., LaMotte, R. H., & Dong, X. (2013). A subpopulation of nociceptors specifically linked to itch. *Nature Neuroscience*, 16(2), 174–182. <https://doi.org/10.1038/nn.3289>
- Haynes, S. E., Hloppeter, G., Yang, G., Kurpius, D., Dailey, M. E., Gan, W. B., & Julius, D. (2006). The P2Y12 receptor regulates microglial activation by extracellular nucleotides. *Nature Neuroscience*, 9(12), 1512–1519. <https://doi.org/10.1038/nn1805>
- Huang, J., Polgár, E., Solinski, H. J., Mishra, S. K., Tseng, P. Y., Iwagaki, N., Boyle, K. A., Dickie, A. C., Kriegbaum, M. C., Wildner, H., Zeilhofer, H. U., Watanabe, M., Riddell, J. S., Todd, A. J., & Hoon, M. A. (2018). Circuit dissection of the role of somatostatin in itch and pain. *Nature Neuroscience*, 21(5), 707–716. <https://doi.org/10.1038/s41593-018-0119-z>
- Imamachi, N., Park, G. H., Lee, H., Anderson, D. J., Simon, M. I., Basbaum, A. I., & Han, S. K. (2009). TRPV1-expressing primary afferents generate behavioral responses to pruritogens via multiple mechanisms. *Proceedings of the National Academy of Sciences of the United States of America*, 106(27), 11330–11335. <https://doi.org/10.1073/pnas.0905605106>
- Inoue, K., & Tsuda, M. (2018). Microglia in neuropathic pain: Cellular and molecular mechanisms and therapeutic potential. *Nature Reviews. Neuroscience*, 19(3), 138–152. <https://doi.org/10.1038/nrn.2018.2>
- Jing, P. B., Cao, D. L., Li, S. S., Zhu, M., Bai, X. Q., Wu, X. B., & Gao, Y. J. (2018). Chemokine receptor CXCR3 in the spinal cord contributes to chronic itch in mice. *Neuroscience Bulletin*, 34(1), 54–63. <https://doi.org/10.1007/s12264-017-0128-z>
- Kashiba, H., Fukui, H., Morikawa, Y., & Senba, E. (1999). Gene expression of histamine H1 receptor in Guinea pig primary sensory neurons: A relationship between H1 receptor mRNA-expressing neurons and peptidergic neurons. *Brain Research. Molecular Brain Research*, 66(1–2), 24–34. [https://doi.org/10.1016/s0169-328x\(98\)00346-5](https://doi.org/10.1016/s0169-328x(98)00346-5)
- Li, J. N., Ren, J. H., Zhao, L. J., Wu, X. M., Li, H., Dong, Y. L., & Li, Y. Q. (2021). Projecting neurons in spinal dorsal horn send collateral projections to dorsal midline/intralaminar thalamic complex and parabrachial nucleus. *Brain Research Bulletin*, 169, 184–195. <https://doi.org/10.1016/j.brainresbull.2021.01.012>
- Liu, X., Wang, D., Wen, Y., Zeng, L., Li, Y., Tao, T., Zhao, Z., & Tao, A. (2020). Spinal GRPR and NPRA contribute to chronic itch in a murine model of allergic contact dermatitis. *The Journal of Investigative Dermatology*, 140(9), 1856–1866. <https://doi.org/10.1016/j.jid.2020.01.016>
- Liu, Y., Abdel Samad, O., Zhang, L., Duan, B., Tong, Q., Lopes, C., Ji, R. R., Lowell, B. B., & Ma, Q. (2010). VGLUT2-dependent glutamate release from nociceptors is required to sense pain and suppress itch. *Neuron*, 68(3), 543–556. <https://doi.org/10.1016/j.neuron.2010.09.008>
- MacDonald, K. P., Palmer, J. S., Cronau, S., Seppanen, E., Olver, S., Raffelt, N. C., Kuns, R., Pettit, A. R., Clouston, A., Wainwright, B., Branstetter, D., Smith, J., Paxton, R. J., Cerretti, D. P., Bonham, L., Hill, G. R., & Hume, D. A. (2010). An antibody against the colony-stimulating factor 1 receptor depletes the resident subset of monocytes and tissue- and tumor-associated macrophages but does not inhibit inflammation. *Blood*, 116(19), 3955–3963. <https://doi.org/10.1182/blood-2010-02-266296>
- McNeil, B. D., Pundir, P., Meeker, S., Han, L., Udem, B. J., Kulka, M., & Dong, X. (2015). Identification of a mast-cell-specific receptor crucial for pseudo-allergic drug reactions. *Nature*, 519(7542), 237–241. <https://doi.org/10.1038/nature14022>
- Miao, X., Huang, Y., Liu, T. T., Guo, R., Wang, B., Wang, X. L., Chen, L. H., Zhou, Y., Ji, R. R., & Liu, T. (2018). TNF-alpha/TNFR1 signaling is required for the full expression of acute and chronic itch in mice via peripheral and central mechanisms. *Neuroscience Bulletin*, 34(1), 42–53. <https://doi.org/10.1007/s12264-017-0124-3>
- Mishra, S. K., & Hoon, M. A. (2013). The cells and circuitry for itch responses in mice. *Science*, 340(6135), 968–971. <https://doi.org/10.1126/science.1233765>
- Nattkemper, L. A., Tey, H. L., Valdes-Rodriguez, R., Lee, H., Mollanazar, N. K., Albornoz, C., Sanders, K. M., & Yosipovitch, G. (2018). The genetics of chronic itch: Gene expression in the skin of patients with atopic dermatitis and psoriasis with severe itch. *The Journal of Investigative Dermatology*, 138(6), 1311–1317. <https://doi.org/10.1016/j.jid.2017.12.029>
- Oetjen, L. K., Mack, M. R., Feng, J., Whelan, T. M., Niu, H., Guo, C. J., Chen, S., Trier, A. M., Xu, A. Z., Tripathi, S. V., Luo, J., Gao, X., Yang, L., Hamilton, S. L., Wang, P. L., Brestoff, J. R., Council, M. L., Brasington, R., Schaffer, A., ... Kim, B. S. (2017). Sensory neurons co-opt classical immune signaling pathways to mediate chronic itch. *Cell*, 171(1), 217–228. <https://doi.org/10.1016/j.cell.2017.08.006>
- Pan, H., Fatima, M., Li, A., Lee, H., Cai, W., Horwitz, L., Hor, C. C., Zaher, N., Cin, M., Slade, H., Huang, T., Xu, X. Z. S., & Duan, B. (2019). Identification of a spinal circuit for mechanical and persistent spontaneous itch. *Neuron*, 103(6), 1135–1149. <https://doi.org/10.1016/j.neuron.2019.06.016>
- Paolicelli, R. C., Bolasco, G., Pagani, F., Maggi, L., Scianni, M., Panzanelli, P., Giustetto, M., Ferreira, T. A., Guiducci, E., Dumas, L., Ragozzino, D., & Gross, C. T. (2011). Synaptic pruning by microglia is necessary for normal brain development. *Science*, 333(6048), 1456–1458. <https://doi.org/10.1126/science.1202529>
- Parkhurst, C. N., Yang, G., Ninan, I., Savas, J. N., Yates, J. R., 3rd, Lafaille, J. J., Hempstead, B. L., Littman, D. R., & Gan, W. B. (2013). Microglia promote learning-dependent synapse formation through brain-derived neurotrophic factor. *Cell*, 155(7), 1596–1609. <https://doi.org/10.1016/j.cell.2013.11.030>
- Pasparakis, M., Haase, I., & Nestle, F. O. (2014). Mechanisms regulating skin immunity and inflammation. *Nature Reviews. Immunology*, 14(5), 289–301. <https://doi.org/10.1038/nri3646>
- Peng, J., Gu, N., Zhou, L., B Eyo, U., Murugan, M., Gan, W. B., & Wu, L. J. (2016). Microglia and monocytes synergistically promote the transition from acute to chronic pain after nerve injury. *Nature Communications*, 7, 12029. <https://doi.org/10.1038/ncomms12029>
- Rao, K. N., & Brown, M. A. (2008). Mast cells: Multifaceted immune cells with diverse roles in health and disease. *Annals of the New York Academy of Sciences*, 1143, 83–104. <https://doi.org/10.1196/annals.1443.023>
- Ringkamp, M., Schepers, R. J., Shimada, S. G., Johaneck, L. M., Hartke, T. V., Borzan, J., Shim, B., LaMotte, R. H., & Meyer, R. A. (2011). A role for nociceptive, myelinated nerve fibers in itch sensation. *The Journal of Neuroscience*, 31(42), 14841–14849. <https://doi.org/10.1523/JNEUROSCI.3005-11.2011>
- Satoh, J., Kino, Y., Asahina, N., Takitani, M., Miyoshi, J., Ishida, T., & Saito, Y. (2016). TMEM119 marks a subset of microglia in the human brain. *Neuropathology*, 36(1), 39–49. <https://doi.org/10.1111/neup.12235>
- Schmelz, M., Schmidt, R., Bickel, A., Handwerker, H. O., & Torebjork, H. E. (1997). Specific C-receptors for itch in human skin. *The Journal of Neuroscience*, 17(20), 8003–8008.
- Shim, W. S., & Oh, U. (2008). Histamine-induced itch and its relationship with pain. *Molecular Pain*, 4, 29. <https://doi.org/10.1186/1744-8069-4-29>
- Simone, D. A., Zhang, X., Li, J., Zhang, J. M., Honda, C. N., LaMotte, R. H., & Giesler, G. J., Jr. (2004). Comparison of responses of primate spinothalamic tract neurons to pruritic and algogenic stimuli. *Journal of Neurophysiology*, 91(1), 213–222. <https://doi.org/10.1152/jn.00527.2003>

- Strakhova, M. I., Nikkel, A. L., Manelli, A. M., Hsieh, G. C., Esbenshade, T. A., Brioni, J. D., & Bitner, R. S. (2009). Localization of histamine H4 receptors in the central nervous system of human and rat. *Brain Research*, 1250, 41–48. <https://doi.org/10.1016/j.brainres.2008.11.018>
- Tozaki-Saitoh, H., Tsuda, M., Miyata, H., Ueda, K., Kohsaka, S., & Inoue, K. (2008). P2Y12 receptors in spinal microglia are required for neuropathic pain after peripheral nerve injury. *The Journal of Neuroscience*, 28(19), 4949–4956. <https://doi.org/10.1523/JNEUROSCI.0323-08.2008>
- Tsuda, M., Kuboyama, K., Inoue, T., Nagata, K., Tozaki-Saitoh, H., & Inoue, K. (2009). Behavioral phenotypes of mice lacking purinergic P2X4 receptors in acute and chronic pain assays. *Molecular Pain*, 5, 28. <https://doi.org/10.1186/1744-8069-5-28>
- Usoskin, D., Furlan, A., Islam, S., Abdo, H., Lönnberg, P., Lou, D., Hjerling-Leffler, J., Haeggström, J., Kharchenko, O., Kharchenko, P. V., Linnarsson, S., & Ernfors, P. (2015). Unbiased classification of sensory neuron types by large-scale single-cell RNA sequencing. *Nature Neuroscience*, 18(1), 145–153. <https://doi.org/10.1038/nn.3881>
- Verge, G. M., Milligan, E. D., Maier, S. F., Watkins, L. R., Naeve, G. S., & Foster, A. C. (2004). Fractalkine (CX3CL1) and fractalkine receptor (CX3CR1) distribution in spinal cord and dorsal root ganglia under basal and neuropathic pain conditions. *The European Journal of Neuroscience*, 20(5), 1150–1160. <https://doi.org/10.1111/j.1460-9568.2004.03593.x>
- Wan, L., Jin, H., Liu, X. Y., Jeffry, J., Barry, D. M., Shen, K. F., Peng, J. H., Liu, X. T., Jin, J. H., Sun, Y., Kim, R., Meng, Q. T., Mo, P., Yin, J., Tao, A., Bardoni, R., & Chen, Z. F. (2017). Distinct roles of NMB and GRP in itch transmission. *Scientific Reports*, 7(1), 15466. <https://doi.org/10.1038/s41598-017-15756-0>
- Wilson, S. R., Gerhold, K. A., Bifolck-Fisher, A., Liu, Q., Patel, K. N., Dong, X., & Bautista, D. M. (2011). TRPA1 is required for histamine-independent, mas-related G protein-coupled receptor-mediated itch. *Nature Neuroscience*, 14(5), 595–602. <https://doi.org/10.1038/nn.2789>
- Yosipovitch, G., Greaves, M. W., & Schmelz, M. (2003). Itch. *The Lancet*, 361(9358), 690–694. [https://doi.org/10.1016/S0140-6736\(03\)12570-6](https://doi.org/10.1016/S0140-6736(03)12570-6)
- Zhuang, Z. Y., Kawasaki, Y., Tan, P. H., Wen, Y. R., Huang, J., & Ji, R. R. (2007). Role of the CX3CR1/p38 MAPK pathway in spinal microglia for the development of neuropathic pain following nerve injury-induced cleavage of fractalkine. *Brain, Behavior, and Immunity*, 21(5), 642–651. <https://doi.org/10.1016/j.bbi.2006.11.003>

SUPPORTING INFORMATION

Additional supporting information can be found online in the Supporting Information section at the end of this article.

How to cite this article: Yang, Y., Mou, B., Zhang, Q.-R., Zhao, H.-X., Zhang, J.-Y., Yun, X., Xiong, M.-T., Liu, Y., Liu, Y. U., Pan, H., Ma, C.-L., Li, B.-M., & Peng, J. (2023). Microglia are involved in regulating histamine-dependent and non-dependent itch transmissions with distinguished signal pathways. *Glia*, 1–18. <https://doi.org/10.1002/glia.24438>